NASA Contractor Report 178306

INTERFACIAL ADHESION OF CARBON FIBERS

Willard D. Bascom

HERCULES, INC.
Hercules Aerospace Division
Magna, Utah

Contract NAS1-17918
August 1987

National Aeronautics and
Space Administration

Langley Research Center
Hampton, Virginia 23665

NASA Contractor Report 178306

INTERFACIAL ADHESION OF CARBON FIBERS

Willard D. Bascom

HERCULES, INC.
Hercules Aerospace Division
Magna, Utah

Contract NAS1-17918
August 1987

National Aeronautics and
Space Administration

Langley Research Center
Hampton, Virginia 23665

INTERFACIAL ADHESION OF CARBON FIBERS

WILLARD D BASCOM*

Introduction

The work reported here was initiated as a result of studies at NASA Langley (NASA Project Code 505-63-01) that indicated low adhesion of carbon fibers to thermoplastic matrix polymers. This problem become apparent in the investigation at the Langley Research Center on the effect of matrix deformation on interlaminar fracture of carbon fiber-polymer matrix composites. Experiments had been planned to fabricate composites with thermoplastic polymers having known failure mechanisms, e.g., crazing, shear banding, etc. The candidate resins included polycarbonate (PC), polyphenylene oxide (PPO), polystyrene (PS), polyetherimide (PEI), and blends of PPO with PS and PC with a polycarbonate-polysiloxane copolymer.

Scanning electron microscopy (SEM) of delaminated composite specimens of PC reinforced carbon fiber (Hercules AS4) suggested poor bonding between fiber and matrix compared to the same fiber in an epoxy matrix. SEM evidence for low adhesion to PC is illustrated in the photomicrographs in Fig. 1.

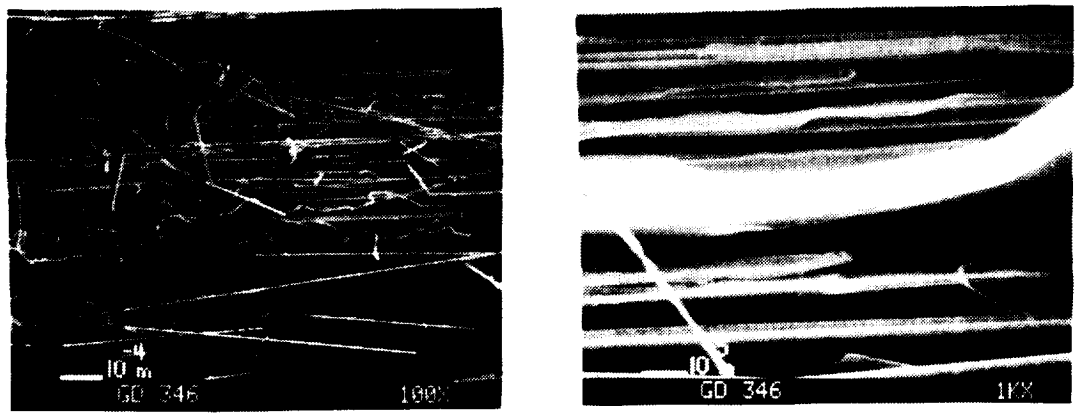

Figure 1. SEM photomicrographs of poycarbonate/AS4 composite fracture surfaces. The matrix appears to have been cleanly stripped from the fibers leaving smooth fibers and curls of deformed polymer.

* Materials Science and Engineering Department, University of Utah

Figure 2. SEM photomicrograph of a polyphenylene sulfide/AS4 composite fracture surface (reference 2).

A similar adhesion problem has been found for AS4 in other thermoplastic polymers such as polyetheretherketone (1) and polyphenylene oxide (PPS). Evidence for low adhesion of AS4 in PPS is presented in the SEM photomicrograph in Fig.2 (2).

Scanning electron microscopy does not provide unequivocal evidence of interfacial failure. Although the fibers appear clean of adhering matrix in Fig. 2, it is possible that they are coated with a thin continuous film of polymer only a few tens of nanometers thick. Depending on the stress conditions, failure can be mechanically focused into the interfacial region but with the locus of failure in the polymer and not at the interface. This situation has been observed in mixed mode adhesive failure (3) and is possible in composite delamination (4).

None the less, the SEM photographs is Figs. 1 and 2 strongly suggest interfacial failure and presumably low adhesion strength between fiber and matrix. Whether or not this was the case needed to be confirmed in order to proceed with the study of delamination micromechanics.

The importance of the bond strength between reinforcement and matrix in composite materials goes beyond the specific problem being addressed in the NASA Langley investigation. Professor M. Piggott (University of Toronto) has put it very succinctly, "the interface is the heart of a composite" (5). The effectiveness of a reinforcement depends in a very fundamental sense on the stress transfer between fiber and matrix and stress transfer is limited by the strength of the "interphase" region which includes the interface, the matrix near the interface, and the outer surface layer of the reinforcement. The weakest of these three locations determines the level of stress transfer. The interphase strength also determines the stress distribution at fiber breaks where the high shear stress concentration (Figure 3) exceeds the interphase strength so that there is local debonding of the matrix from the fiber for some distance from the fiber end. This debonding, or shear lag , relieves the stress concentration which otherwise might initiate failure of the composite. Stress transfer and shear lag effects have been extensively discussed in the literature (6-9) for uniaxial tensile strength. Stress transfer in delamination is not well understood and needs to be examined.

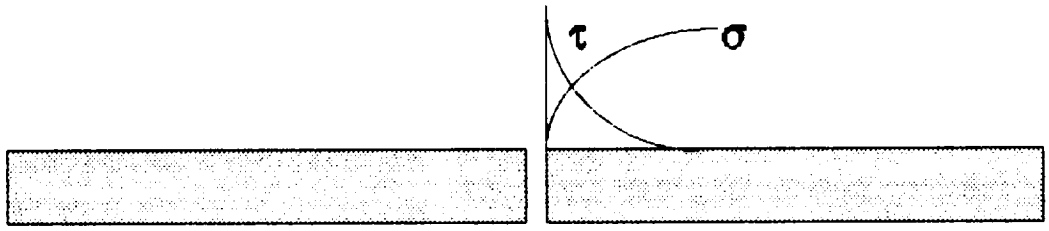

Figure 3. Stress distribution at a fiber break

OBJECTIVE

The purpose of the work reported here was to determine the adhesion strength of AS4 fibers to thermoplastic polymers; specifically to polycarbonate, polyphenylene oxide, polyetherimide, polyphenylene oxide blends with polystyrene, and polycarbonate blends with a polycarbonate-polysiloxane copolymer. Data are also included for polysulfone. It was recognized at the outset, as explained in the next section, that an absolute measure of the fiber matrix adhesion would be difficult. However, it is feasible to determine the fiber bond strengths to the thermoplastics relative to the bond strength of the same fibers to epoxy polymers.

It was anticipated, and in fact realized, that the adhesion of AS4 to the thermoplastic polymers was relatively low. Therefore, further objectives of the study

were to identify means of increasing fiber/matrix adhesion and to try to determine why the adhesion of AS4 to thermoplastics is significantly less than to epoxy polymers

APPROACH

The bond strength between fiber and matrix can be measured using the embedded single filament tensile test (10-15). The test is conducted by embedding a single carbon filament in a micro-tensile specimen of the matrix polymer As shown schematically in Fig 4, the specimen is stressed until the fiber is completely fragmented

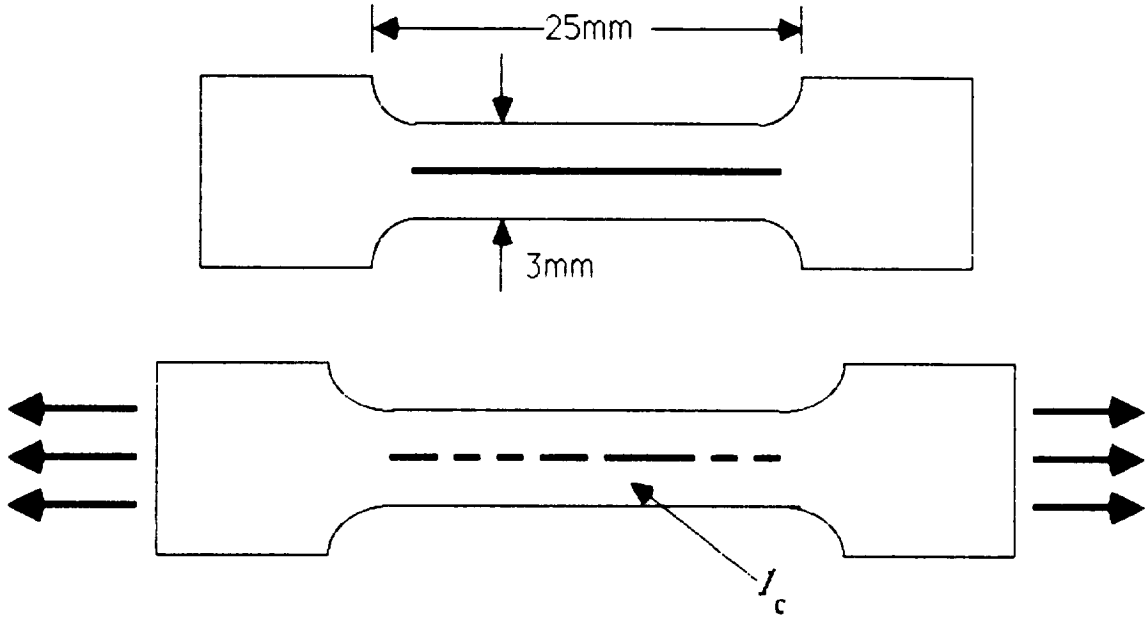

Figure 4 Schematic of embedded single filament specimen Under tensile loading the filament fragments until reaching the critical length, l_c

The minimum fragment length, l_c, is related to the fiber tensile strength, σ_c, diameter d, and the shear strength, τ_c, between the fiber and matrix. In the ideal case of a filament with a uniform strength, the fragment length is given by (9):

$$\ell_c = \frac{\sigma_c}{2} \frac{d}{\tau_c} \qquad [1]$$

However, the strength of carbon fibers has a broad statistical distribution (Fig. 5) so that equation 1 takes the form (12);

$$\ell_c = \frac{d}{2\tau_c} \sum \sigma_c \qquad [2]$$

Where:

$$\sum \sigma_c \qquad [3]$$

represents some statistical distribution of σ_c. Equation 2 can be rearranged to:

$$\tau_c = \frac{d}{2\ell_c} \sum \sigma_c \qquad [4]$$

which relates the bond strength to the critical length and the critical aspect ratio, ℓ_c/d. If it is assumed that the fiber diameter is constant then the critical length or critical aspect ratio are inversely proportional to the fiber/matrix bond strength. As will be shown later, this is a reasonable assumption. It must also be assumed that the fiber strength distribution is constant. This is reasonable for one fiber type, e.g., AS4, and if the fragment lengths are comparable. In this study these requirements are not rigorously meet. Fortunately, the conclusions from the critical length measurements are supported by the birefringence observations as discussed later.

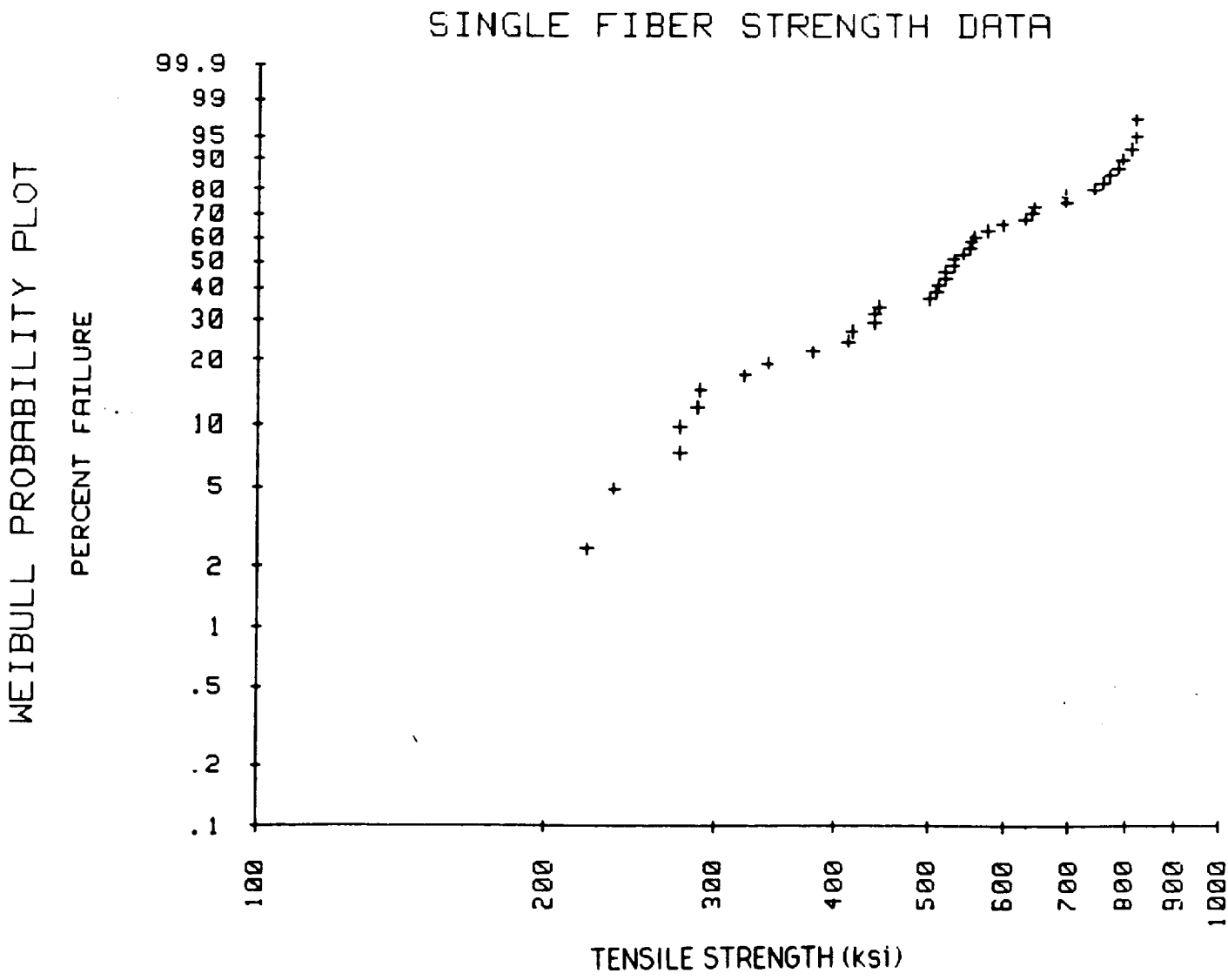

Figure 5. Weibull probability plot of AS4 single filament tensile strength data. Note that data points tend to cluster into groups which suggests discrete flaw strengths

Ideally, one would wish to determine, τ_c, the boundary shear strength but this requires some measure of the fiber strength and the appropriate form of $\Sigma \sigma_c$ is problematical. Drzal (12) measured an average fiber strength for gauge lengths of ℓ_c using a microtensile test machine (16). This particular device is no longer commercially available and would be inordinately expensive to build.

The embedded single filament test yields further information about fiber/matrix adhesion if the matrix polymer is transparent and stress birefringent.

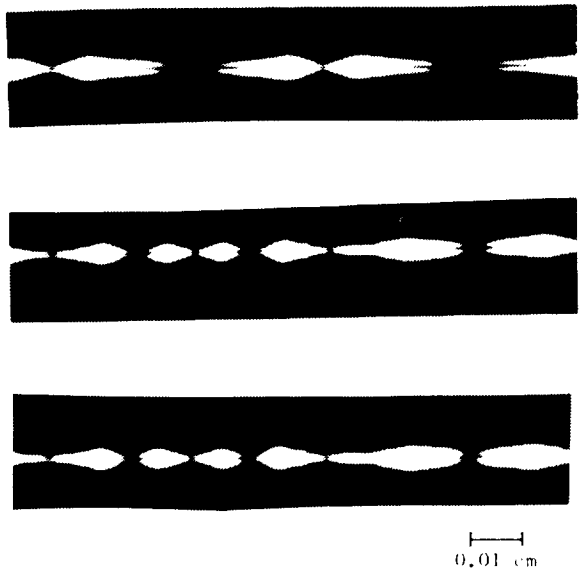

Figure 6. Stress birefringence patterns at fiber breaks characeristic of strong adhesion (AS4 in epoxy) A-C change in pattern with increasing stress (reference 14)

Viewing the specimen between crossed polarizing filters, the high shear stress at fiber breaks produces a bright birefringence pattern The sequence of photographs in Fig. 6 shows the development of stress birefringence with increasing tensile stress for a single carbon filament in an epoxy polymer. As the fiber begins to fragment, symmetrical bright birefringence nodes develop immediately at the breaks (Fig 6A) With increasing stress these nodes move away from the fiber ends but leave a more or less uniform sheath of birefringence around the fiber (Fig. 6B) This sequence of patterns is observed when there is strong bonding between fiber and matrix (12,14)

A different sequence of patterns occur when the bond between fiber and matrix is weak. As shown in Fig. 7A, symmetrical birefringence nodes develop at the initial fiber breaks as in the case of strong bonding However, with increasing tension, these nodes recede from the fiber ends leaving a relatively indistinct sheath of birefringence as shown in Fig 7B The intensity of this sheath seems to be proportional to the bond strength and when the bond strength is low the movement of the nodes is very rapid and suggests an "unzipping" of the matrix from the fiber These observations are further illustrated and discussed in the Results section

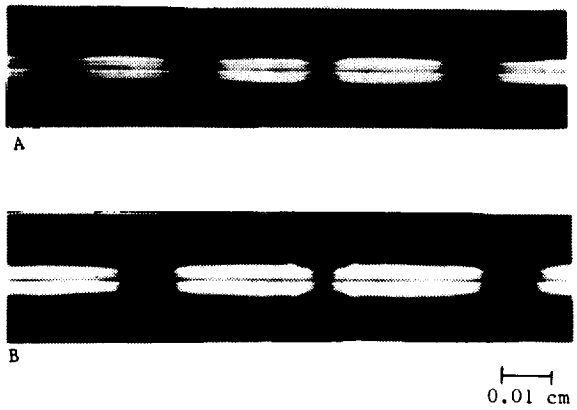

Figure 7. Stress birefringence patterns at fiber breaks characteristic of low adhesion (SiC in epoxy). A-B, change in pattern with increasing stress (reference 14)

Another distinction between strongly and weakly bonding systems is the relaxation behavior of the birefringence patterns. In the case of strong bonding, release of the tension on the specimen causes the birefringence nodes to disappear as shown in Fig 8 but the sheath that formes when the nodes recede from the fiber ends persists indefinitely (Fig 8B). Specimens left unstressed for as long as 3yrs still exhibited the birefringent sheath. On the other hand, weakly bonded systems show a complete relaxation of the birefringence, as shown in Fig 9. The persistence of the birefringence in the case of strong bonding has been interpreted as shear yielding of the matrix in the vicinity of the fiber breaks: the fiber/matrix adhesion strength is stronger than the yield strength of the polymer(14). The complete relaxation of the birefringence is interpreted as indicating interfacial failure; the sheath as well as the nodes are due to elastic shear stresses that relax when the tension on the specimen is removed

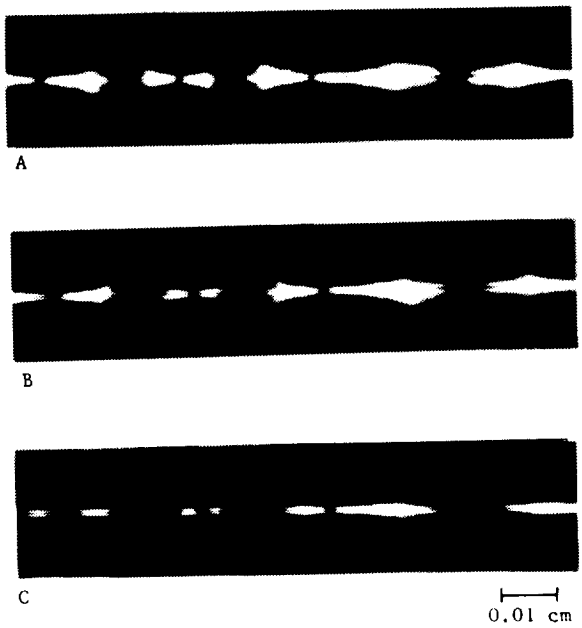

Figure 8. Stress birefringence relaxation when load is removed from single filament specimens. Strong adhesion. AS4 in epoxy (reference 14)

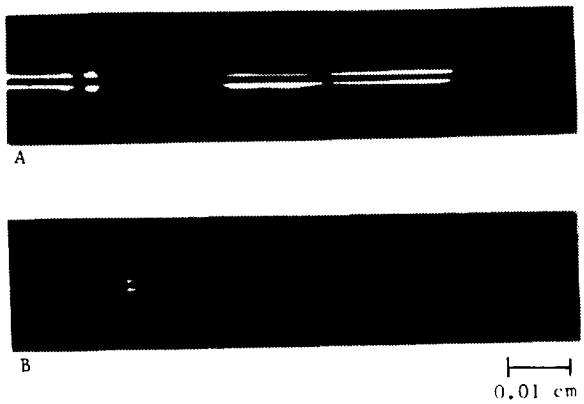

Figure 9. Stress birefringence relaxation when load is removed from a single filament specimen. Low adhesion. SiC in epoxy (reference 14)

It should be noted that in these single fiber tests, a significant thermally induced compressive strength normal to the interface can develop which measurably increase the bond strength above the inherent adhesion strength between fiber and matrix(16). This effect is illustrated in the Results section. Comparable compressive stresses do not develop in a composite with a realistic fiber volume of 60-65%.

EXPERIMENTAL

SPECIMEN PREPERATION: The technique for preparing and testing imbedded single carbon filament/epoxy specimens has been describe elsewhere (14) Briefly, a filament is positioned in a silicone mold as shown in Fig. 10 The mold is carefully filled with liquid epoxy resin avoiding inclusion of air bubbles. The assembly is cured and the specimen is clamped into a micro-tensile test fixture (Fig 11) that fits on the stage of a transmission light microscope.

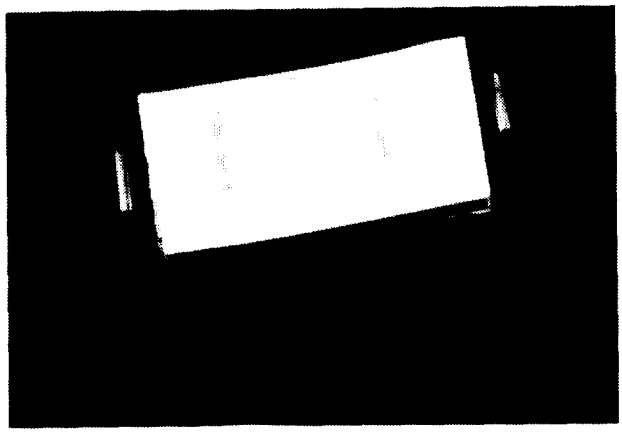

Figure 10. Silicone mold for epoxy specilmens. Filament is positioned lengthwise through the mold cavity

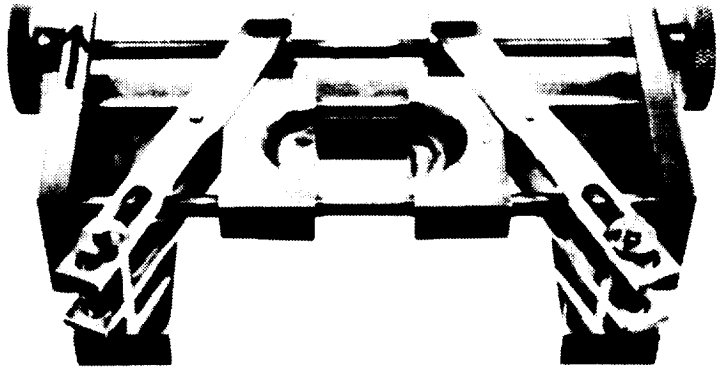

Figure 11 Microtensile tester (reference 14)

A different technique was used to prepare specimens of carbon filaments in the thermoplastic polymers since it would involve injection molding to make specimens similar to the epoxy specimens. Instead, a single filament was placed lengthwise on a thin plate of the polymer, Fig 12. The filament was then coated with a film of the same polymer dissolved in a volatile solvent

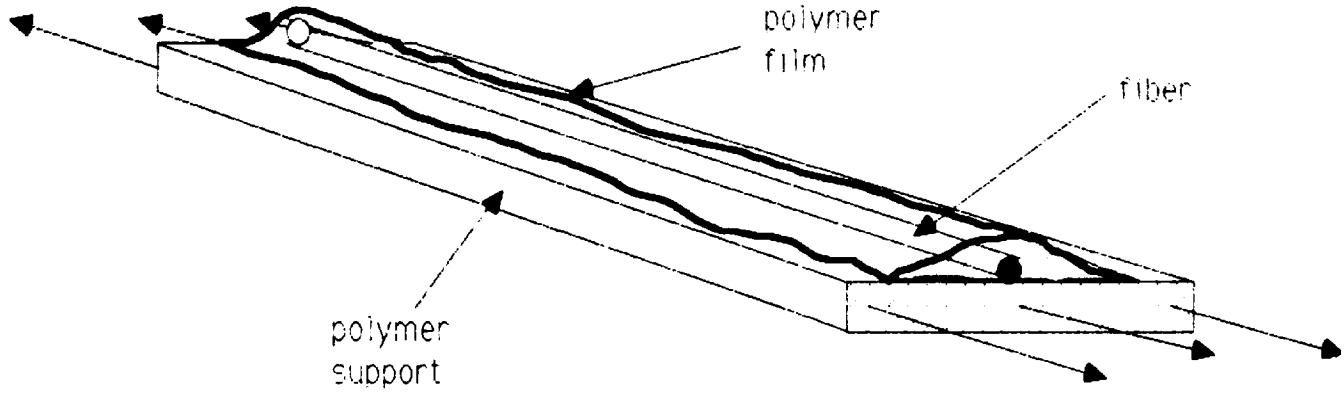

Figure 12. Schematic of specimen used to test single carbon filaments in thermoplastic polymers. The support plate is 12.5mm wide, 37.5 mm long and 6.25 mm thick

A series of experiments were conducted to determine the drying conditions for complete removal of the solvent from the coating. The coatings are thin, 25 mm and the solvents, methylene chloride (MeCl) and dichloroethane (DCE), are highly volatile so that evaporation was essentially complete within 24hrs at 25°C. To insure complete removal of the solvent, the films applied from MeCl were dried at 75°C for 8hrs and films applied from MeCl/DCE mixtures were dried at 81°C for 16hrs. The criterion used for complete removal of the solvent was that the fragment length, l_c, was not reduced by further drying at these conditions. Drying at higher temperatures caused the development of residual compressive stresses as discussed in Appendix A. Drying at 75°C and 81°C were compromise conditions to insure complete solvent removal without the development of large compressive stresses. As shown in the Appendix, the compressive stress developed around the carbon fibers in the thermoplastics dried at 75°C and 81°C was about the same as the stress on the carbon fiber in the epoxy polymers.

The test procedure was modified for the PPO-PS and the PC-PC/polysiloxane experiments since these materials could not be readily obtained in the form of 6mm sheets from which to cut the support plate (Fig 12) Instead, a PC support plate was used which was first coated with a film of the test polymer The fiber was then positioned on the dried film and coated There was no evidence of debonding of the film from the PC support in these experiments Also, critical length measurements were made for AS4 fiber embedded in PPO on both PPO support plates and PC plates prefilmed with PPO There were no significant differences in the critical length

It was found that the procedure used to clean the support plate had a significant effect on the critical length At first the plates were simply washed in an aqueous detergent solution Later is was found that the critical length was reduced by following the detergent wash with a light polishing on a metallographic wheel in a dilute slurry of alumina powder The alumina powder is a powerful adsorbing agent so it is assumed (although not proven) that it adsorbed detergent or other surface active materials on the support plate that otherwise migrated to the fiber/ polymer interface

The effect of the film coating thickness on the critical length was also investigated because of possible effects of the upper surface of the film on filament fragmentation It was found that a film coating of less than a fiber diameter .7mm was sufficient However, in practice the fiber was always embedded at least two fiber diameters below the surface of the coating film

The critical length was determined by tensile stressing a specimen until the filament was completely fragmented The stress interval over which fiber breakage was complete was usually narrow so that there was little difficulty in determining when fragmentation was complete The critical lengths exhibited a broad statistical distribution as shown in Fig 13 for a single specimen This wide distribution in l_c reflects the statistical distribution in the fiber strength (Eq 2 and Fig 5) In order to obtain a statistically significant measure of the critical length, 10-12 specimens were tested for each test condition and the data combined as shown in Fig 14 The data were analyzed using normal, log-normal and Weibull statistics All of these distributions gave essentially the same mean values and variances The data reported here were obtained using the normal distribution function

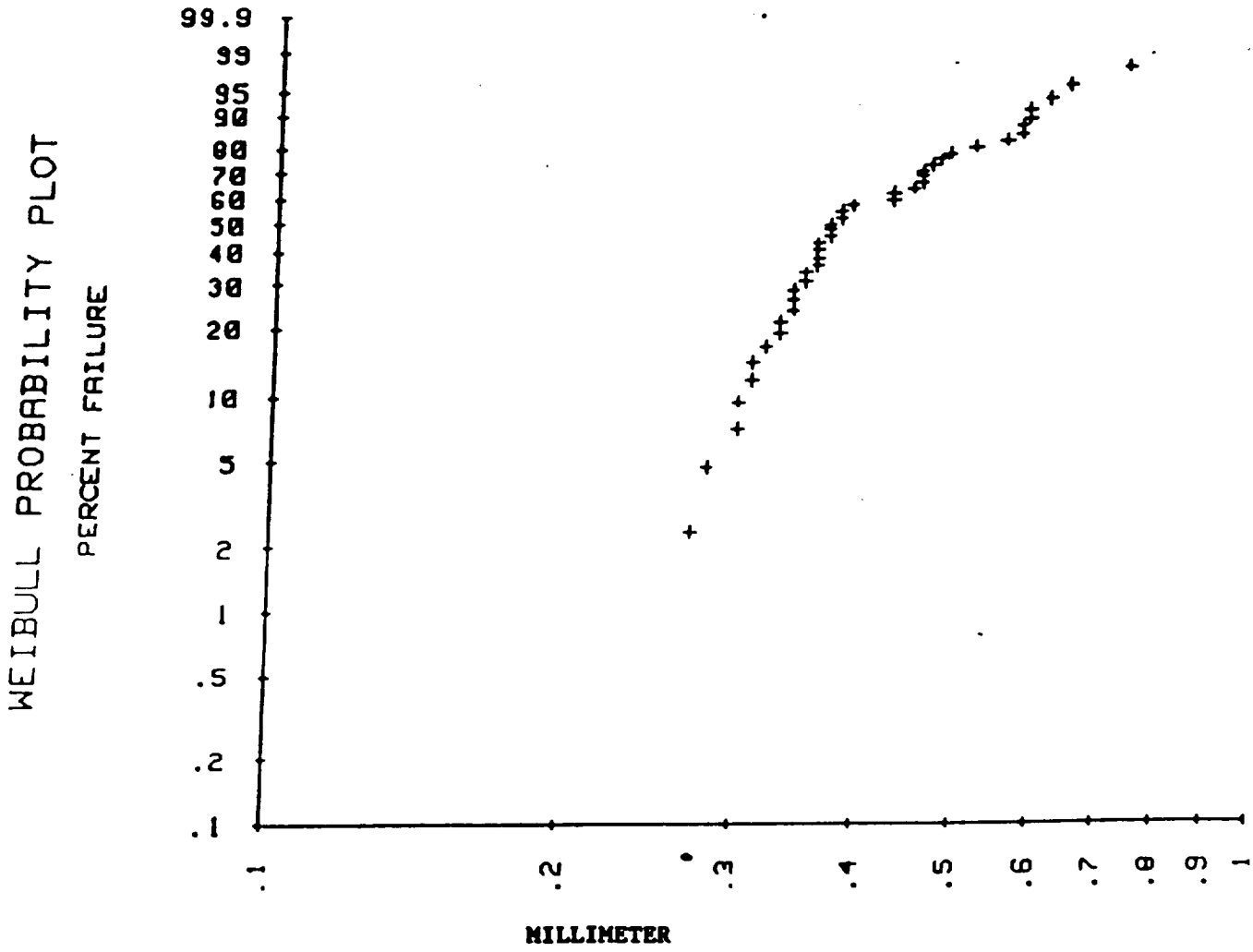

Figure 13. Weibull distribution of l_c data for one specimen (AS4 in epoxy) Note the discontinuous distribution of fragment lengths similar to the distribution of fiber tensile strengths (Fig 5)

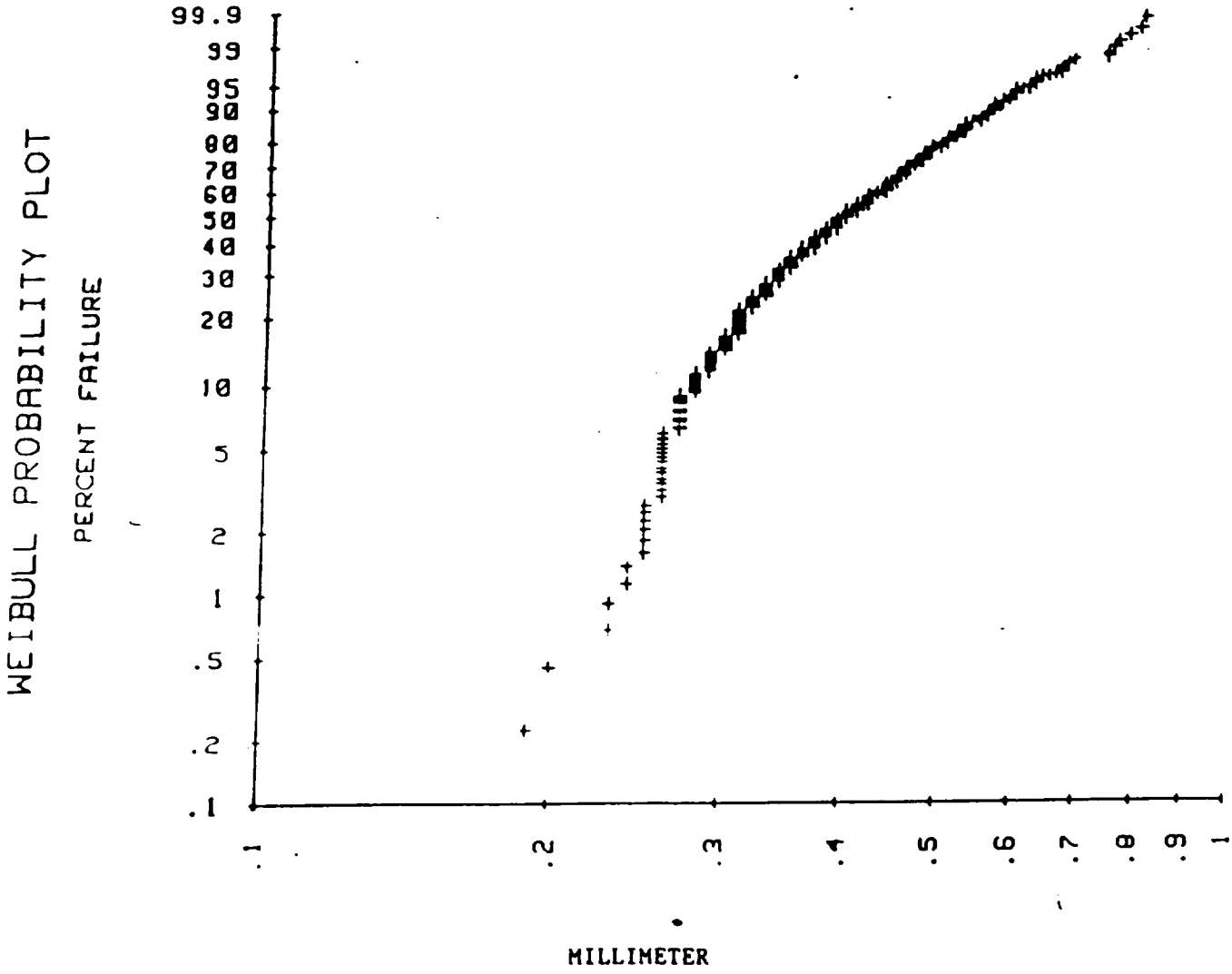

Figure 14. Weibull distribution of combined /c data for ten specimens.

FIBER SURFACE MODIFICATION; Various sizing agents were applied to the carbon fiber as well as variations in surface treatment. The distinction between surface treatment and sizing needs to be emphasized. Commercially produced carbon fibers are given a surface treatment immediately after the final carbonization/graphitization operation. The surface treatments vary for different manufactures and are generally a chemical oxidation As discussed in reference 18 the treatment also involves a cleaning of the fiber of residual material left on the fiber during the high temperature processing as well as some modification of the surface chemical constitution.

Sizing is a deliberate coating of the fiber usually with a film forming polymer composition to aid processing and sometimes to enhance mechanical properties. Commercial coatings are usually applied in an attempt to reduce fiber damage during prepreging and filament winding. In this study sizings were applied in an attempt to improve adhesion. The apparatus used is shown schematically in Fig 15

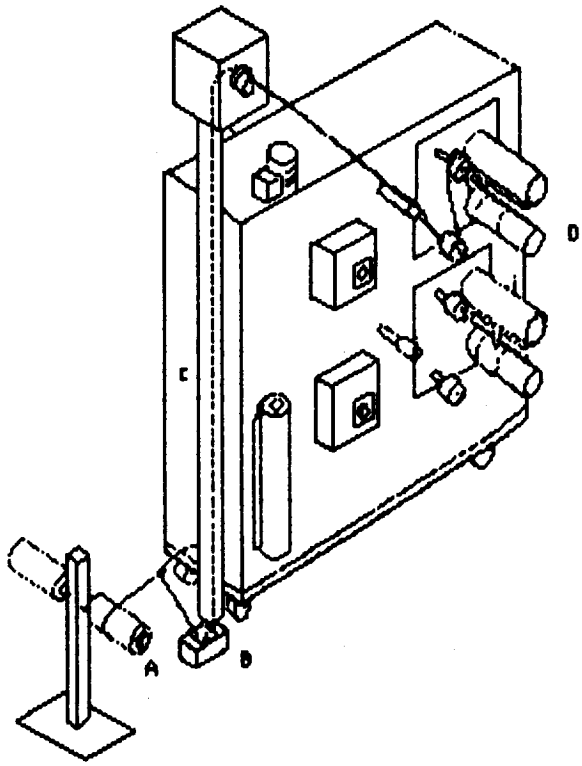

Figure 15. Apparatus used to size carbon fiber tows. A, fiber spool; B,sizing bath; C, drying tower; D, take-up drive

The amount of sizing applied to the fiber (sizing level) was controlled by the bath concentration, the speed of the fiber tow and the temperature in the drying tower. The sizing level was measured by solvent extraction with methylene chloride.

The effect of varying the intensity of the fiber surface treatment on adhesion was studied. The treatment level was set above and below the level used by Hercules for commercial carbon fiber products, nominally 100%. Levels of 0% (unsurface treated fiber designate as AU4), 50%, 100% (normal condition), and 400% were tested. The actual treatment conditions are Hercules proprietary information. The fiber was treated in a pilot plant facility using AU4 from production.

SURFACE ANALYSIS. Surface spectroscopy and wettability measurements were used to characterize the AS4 and other carbon fibers. X-ray photon spectroscopy (XPS) analysis was performed by Surface Science Laboratories (Mountain View, CA). Contact angle measurements were made using a Wilhelmy tensiometer (Rame' Hart, Mountain Lakes, NJ). This technique involves measuring the force on a single carbon filament as it is immersed and emersed through the surface of a liquid as shown schematically in Fig. 16.

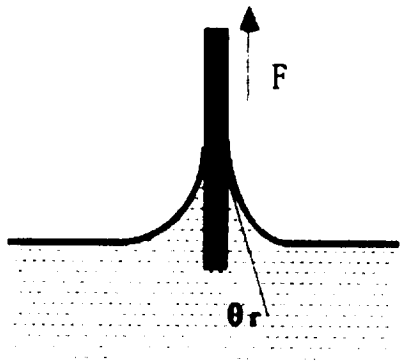

Figure 16. Schematic of the meniscus force on a filament being pulled through the surface of a wetting test liquid. θ is the receding contact angle.

The emersion (or immersion) force (F) is related to the receding (or advancing) contact angle (θ) by,

$$F = \pi d \gamma_{LV} \cos\theta \qquad [5]$$

where γ_{LV} is the surface tension of the wetting liquid. The tensiometer output is in mass units (m) so that the contact angle is given by:

$$\cos\theta = ma/\pi d \gamma_{LV} \qquad [6]$$

where a is the gravitational constant (980.1 cm/sec) The boyancy correction is negligible for small diameter fibers. $d < 20\ \mu m$.

The carbon filament was mounted on the electrobalance (Cahn Instruments. Cerritos, CA) using a wire stirrup as shown in Fig. 17.

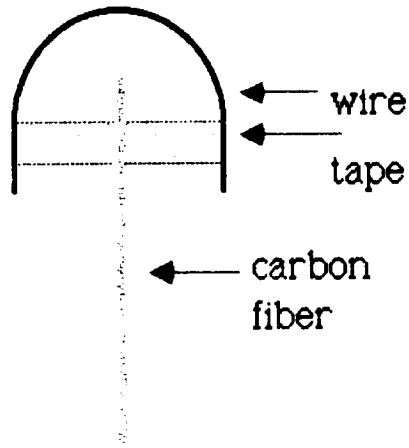

Figure 17. Single filament mounted on a wire stirrup

It was found that some adhesive tapes are sufficiently hygroscopic so that when the specimen and holder were held just above the water surface there was a measurable increase in weight. Through trial and error, a tape was found that did not absorb any detectable amount of water over the duration of the test which in some instances was as

long as ten minutes

The specimen weight was electronically counter balanced so that the measured weight was due only to the immersion or emersion force which could be measured to 0.5 μg

THERMAL DESORPTION The gaseous products that evolve from heated carbon fiber samples were analyzed using mass spectroscopy (MS). The heating rate was 25°C/ min up to 310°C followed by a hold at 310°C for 5 min. The total organic materials evolved over the heating range was recorded along with the output at mass 44 (CO_2), mass 57 (straight chain hydrocarbon) and mass 149 (carbonyl fragments).

Tows of carbon fiber were heat treated to remove thermally desorbable specie by passing the tows through a tube furnace at 750°C. The furnace was flushed with nitrogen gas and the residence time was 90sec

RESULTS AND DISCUSSION

EMBEDDED SINGLE FILAMENT TESTS

The tensile properties and diameter of the carbon fibers studied are listed in Table I.

TABLE I

Carbon Fiber Properties

Fiber designation	Diameter d, μm	0° Laminate Tensile Properties Strength ksi/MPa	Modulus Msi/GPa	Elongation %
AS1[a]	8.0	450/3103	33/228	1.32
AS4[a]	6.84	520/3587	34/235	1.53
XAS[b]	6.64	500/3447	33/230	1.67

[a]Hercules Inc

[b]Grafil Hysol

The properties of the epoxy polymers are given in Table II

TABLE II
Properties of Epoxy Polymers

Designation	Epoxide	Curing agent	Tensile Properties Strength ksi/MPa	Modulus ksi/MPa
828/m-PDA	Shell 828 (DGEBA)	metaphenylene diamine	5.8/40	523/3620
828/D230	Shell 828 (DGEBA)	Jeffamine D230 (polyoxypropylene amine)	9.3/64	379/2614

DGEBA = diglycidylether of bisphenol A

The properties of the thermoplastic polymers are listed in Table III along with the solvent and drying conditions used to apply the films over the carbon filament

TABLE III
Mechanical Properties of the Thermoplastic Polymers

Polymer Properties	Drying Conditions		Tensile	
	solvent	time/temperature	strength ksi/MPa	modulus ksi/MPa
polycarbonate	methylene chloride	24hr/25°C 16hr/75°C	9.5/65	345/2400
polyphenylene oxide	methylene chloride/dichloro-ethane 1/1 wt ratio	4hr/25°C 16hr/81°C	7.0/48	325/2200
polyetherimide[a]	methylene chloride	4hr/25°C 16hr/75°C	15.2/105	430/2965
polysulfone[b]	methylene	24hr/25°C 16hr/75°C	10.1/70	365/254

polystyrene/ polyphenylene oxide (25/75 wt ratio)	methylene chloride/dichloro-ethane, 1/1 wt. ratio	4hr/25°C 24hr/81°C	-----	-----
polycarbonate/ polycarbonate-polysiloxane copolymer[c] (7.5/92.5 wt ratio)	methylene chloride	24hr/25°C 16hr/75°C	-----	-----

[a]Ultem, General Electric Corp.
[b]Udel, Union Carbide Corp
[c]Copel 3220, General Electric Corp

The critical lengths and critical aspect ratios measured for the carbon fibers in the different polymers are given in Tables IV - VII

TABLE IV
Critical Aspect Ratio for Carbon Fiber/Epoxy Systems

Carbon Fiber	Epoxy	Critical Lengths mm	Critical Aspect Ratio, ℓ_c/d mean	99% confidence limits on the mean
AS1[a]	828/mPDA	0.3	42	----------
AS4	828/mPDA	0.38	55	53 - 57
AS4	828/D230	0.41	60	58 - 62
XAS	828/m-PDA	0.21	32	31 - 33

[a] Reference 12

TABLE V

Critical Aspect Ratio for AS4 in Thermoplastic Polymers

Matrix	Critical Lengths mm	Critical Aspect Ratio, ℓ_c/d mean	99% confidence limits on the mean
polycarbonate	0.74	108	101-115
polyphenylene oxide	0.83	121	115-125
polyetherimide	0.64	93	90-96
polysulfone	0.83	121	114 - 128
PPO/PS (75/25)[a]	1.41	206	193 - 218
PC/PC-polysilicone(92.5/7.5)[a]	1.01	148	-----

[a]wt.%

TABLE VI

Critical Aspect Ratio for AS1 in Thermoplastics

Matrix	Critical Lengths mm	Critical Aspect Ratio, ℓ_c/d mean	99% confidence limits on the mean
polycarbonate	0.95	119	114 - 124
polyetherimide	0.67	84	80 - 88

TABLE VII

Critical Aspect Ratio for XAS in Thermoplastic Polymers

Matrix	Critical Lengths mm	Critical Aspect Ratio, ℓ_c/d mean	99% confidence limits on the mean
polycarbonate	0.36	54	52 - 56
polyphenylene oxide	0.37	55	53 - 58
polyetherimide	0.36	55	52 - 57
PPO/PS (75/25)[a]	0.41	61	58 -64
PPO/PS (70/30)[a]	0.43	--	---
PC/PC-silicone (92.5/7.5)[a]	0.66	--	---

[a]wt.%

The critical lengths and aspect ratios are clearly greater for AS4 and AS1 in the thermoplastics than in the epoxy polymers. On the other hand, the critical lengths and aspect ratios for the XAS fiber in the thermoplastics are lower than for the other two fibers and closer to the value for XAS in an epoxy.

The birefringence patterns for AS4 in polycarbonate are presented in Fig. 18 as a sequence of photographs that show the development of stress concentration nodes at the initial breaks (Fig 18A), the receding of the nodes from the break with a slight increase in stress (Fig 18B), and the decay of the birefringence when the stress on the specimen was released (Fig 18C). This same sequence was observed for both AS4 and AS1 in all of the thermoplastics.

These birefringence patterns are indicative of low adhesion; the facile recedence of the initial node suggest an "unzipping" of the matrix from the fiber, and the nearly complete disappearance of the birefringence on removing the stress on the specimen.

Taken together, the high ℓ_c and ℓ_c/d and the sequence of birefringence patterns are strong indications of low adhesion of AS1 and AS4 to the thermoplastics.

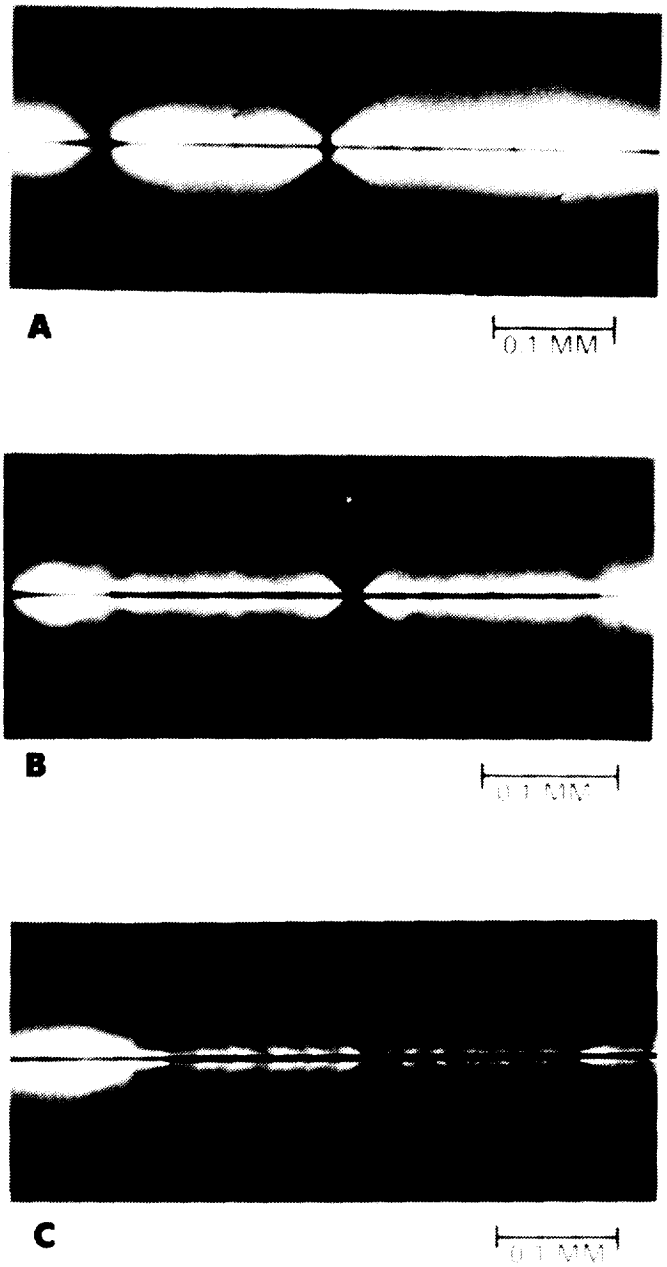

Figure 18. Stress birefringence patterns for AS4 in polycarbonate.

certainly compared to their adhesion to the epoxy polymers

On the other hand, the XAS exhibited shorter critical lengths and critical aspect ratios which suggest good adhesion to the thermoplastics as well as to the epoxy. The birefringence patterns shown in Fig 19 also indicate strong adhesion: the receding nodes leave a strong birefringent sheath (Fig 19B)

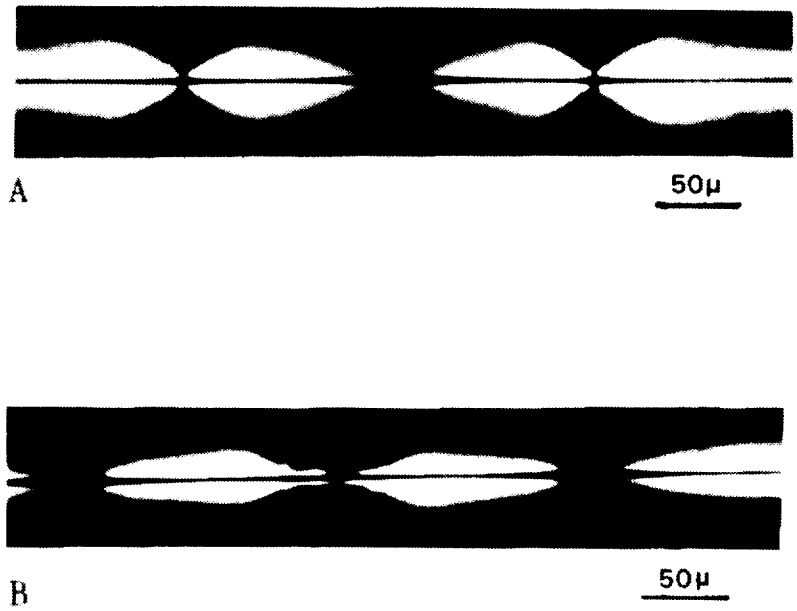

Figure 19 Stress birefringence patterns for XAS in polycarbonate

POLYMER BLENDS. The embedded filament tests of mixtures of polyphenylene oxide with polystyrene were characterized by extensive cracking of the coating film This microcracking is illustrated in Fig 20 for 30wt% of PPO in PS At low magnification (Fig 20A) microcracking appeared to be random through the coating At high magnifications, there was a subset of short microcracks initiating from the fiber/matrix boundary (Fig 20B). Increasing the PPO concentration to 70wt% suppressed general cracking of the coating but microcracks were evident at and near fiber breaks. Fig 21

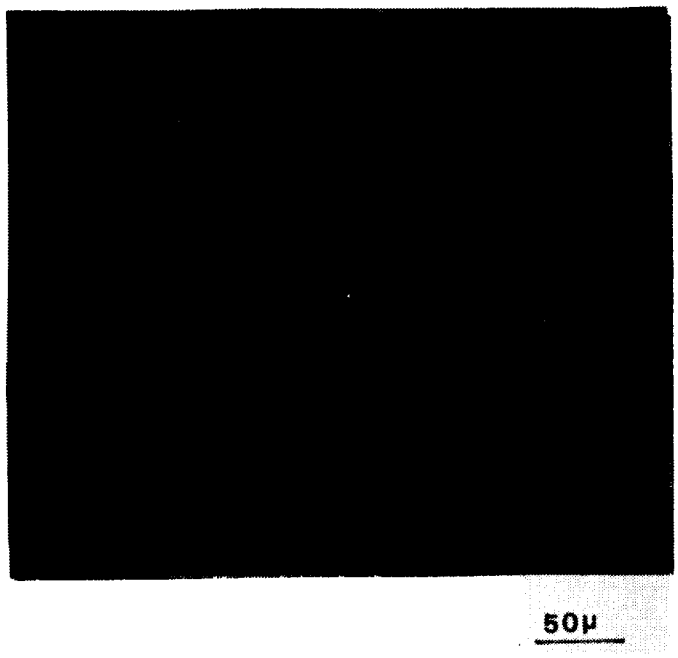

Figure 20A General microcracking of a polystyrene coating

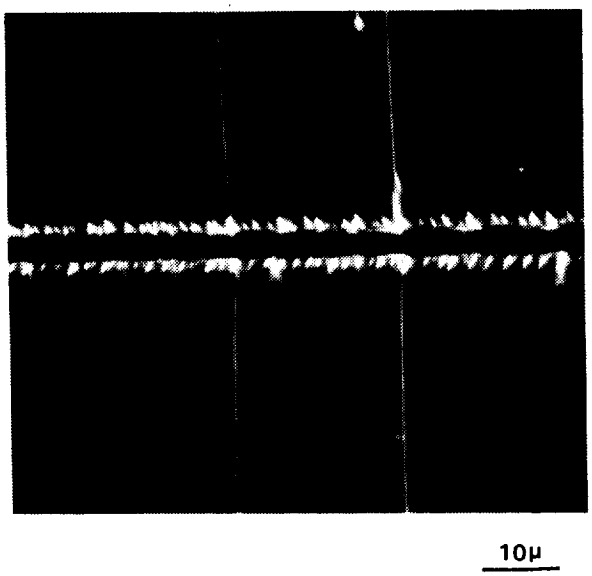

Figure 20B Surface microcracking along an AS4 fiber in polystyrene

Figure 21 Microcracking at a break in an AS4 fiber in PPO/PS (75/25) The central crack is located at the fiber break The cracks left and right of center are at the terminal points of the debonding between fiber and matrix

The loss in stress continuity in the coating film as in Fig 20A, clearly obviated any meaningful critical length determination Even localized cracking, as in Fig 20B, may effect stress transfer

The critical lengths of both AS4 and XAS in blends of polycarbonate with the polycarbonate-polysiloxane copolymer (PC/PC-silicone) were relatively high Table V and Table VII Quite possibly the PC-silicone copolymer is adsorbed or deposited on both fiber types and acts to reduce fiber-matrix interfacial energy or form a weak boundary layer The photomicrograph in Fig 22 shows the birefringence at a fiber break in this polymer blend The birefringence is diffuse due to light scattering by the PC-silicone particles Some particles appear to be attached to the fiber surface

Figure 22. The stress birefringence for XAS in a PC/PC-siloxane blend. Note the PC-siloxane particles which at higher magnification can be seen at the fiber matrix boundary.

SIZINGS Various sizings were applied to AS4 in an attempt to improve adhesion to polycarbonate. The results of these tests are presented in Table VIII. All of the sizings were applied from methylene chloride except the aminopropyl silane which was applied from aqueous solution. Each sizing was applied at various loadings ranging from 0.05-1.0%. The data presented in Table VIII represent the lowest ℓ_c (best adhesion) measured which in some cases was greater than the control, e.g., the sizing reduced the adhesion.

Only the phenoxy** sizing significantly increased the AS4/polycarbonate adhesion. The best results were obtained for sizing levels less than 0.1wt %. The birefringence pattern generally indicated good adhesion although this varied along the filament in a given specimen and between specimens. It is quite possible that the sizing was not evenly distributed on the fiber (or through the tow) and that better control of the sizing operation might improve adhesion still further.

TABLE VIII

Effect of Sizings on the Adhesion of AS4 to Polycarbonate

Sizing Agent	wt % on fiber	Critical Length mm	Critical Aspect Ratio ℓ_c/d mean	99% Confidence Limits on the mean
none	---	0.74	108	101 -115
W-size[a]	1.0	0.64	94	91 -98

** The phenoxy sizing was suggested by Prof. L.T. Drzal, Michigan State University.

epoxy-anhydride[b]	0.45	0.78	114	110 - 118
polyimide[c]	0.25	1.07	156	145 - 167
amino-propylsilaned	0.12	0.68	99	94 - 103
polycarbonate	0.1	0.78	115	110 - 119
phenoxy[e]	0.08	0.54	79	77 - 81

a. Hercules proprietary epoxy-based size
b diglycidylether Bisphenol A/hexahydrophthalic anhydride
c. proprietary sizing supplied by NASA
d A-1100. Union Carbide Corp
e PKHC Union Carbide Corp

SURFACE TREATMENT The effect of surface treatment on the adhesion of the carbon fibers to PC is presented in Table IX. Normal surface treatment increased adhesion of the AS4 and XAS but surface treatment beyond the normal level actually decreased adhesion Intermediate surface treatment variations of the AS4 were tried but without effect.

TABLE IX
The Effect of Surface Treatment on the Adhesion of AS4 to Polycarbonate

Fiber	Surface Treatment Level	Critical Length. mm
AU4	none	0.86
AS4	normal	0.74
AS4	4X	0.89
AU1	none	0.90
AS1	normal	0.95
XAU	none	0.57
XAS	normal	0.36

WEAK BOUNDARY LAYER. The presence of a weak boundary layer is often the cause of low adhesion. There are at least two ways in which a weak boundary layer might develop at the carbon fiber/thermoplastic interface. First, there may be low molecular weight (MW) components in the polymer which migrate to the interface. Second, there could be low MW components on the fiber surface formed during oxidation and carbonization which are not removed in the surface treatment process.

The possibility of low MW components in the polycarbonate was addressed by fractionating the polymer using size exclusion chromatography. The chromatogram for the unfractionated PC is given in Fig 23 and clearly shows low MW materials which were removed by fractionation (Fig 24). However, the critical lengths for AS4 in the fractionated polycarbonate were not significantly different than for the unfractionated PC. TableX.

TABLE X
Effect of Polycarbonate Fractionation on AS4 Critical Length

Polycarbonate	Critical Length mm	Critical Aspect Ratio ℓ_c/d	
		mean	99% confidence limits on the mean
as received	0.74	108	101-115
fractionated	0.81	133	110-124

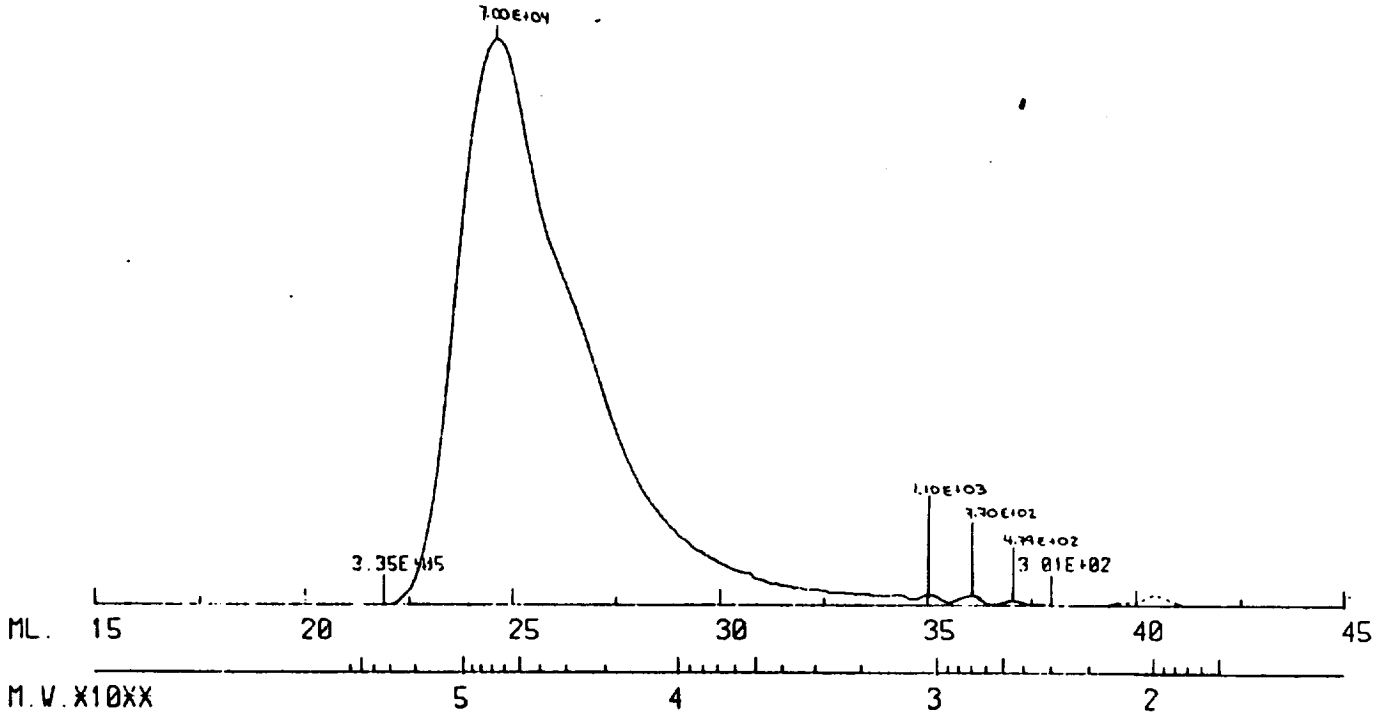

Figure 23. Size exclusion chromatogram of unfractionated polycarbonate

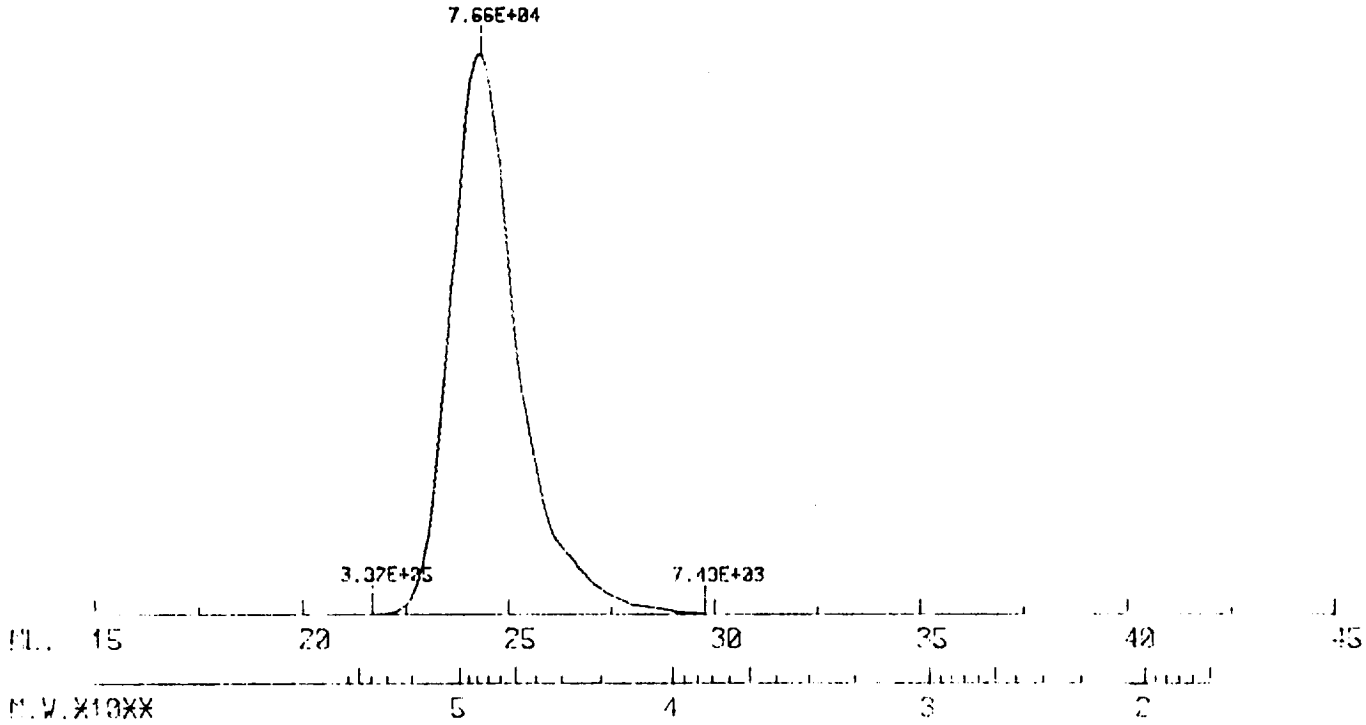

Figure 24. Size exclusion chromatogram of fractionated polycarbonate Note removal of components with MW below 10^4 (compare with Fig 23)

To test for the possibility of low MW contaminants on the AS4 fiber, a tow of AS4 fiber was heat treated by passing through a furnace at 750°C and by soxlet extraction with tetrahydrofuran(THF) As shown in Table XI, neither the heat treatment or the solvent extraction improved the adhesion of AS4 to polycarbonate

TABLE XI
Effect of Solvent Extraction and Heat Cleaning on the Critical Length of AS4 in Polycarbonate

Treatment	Critical Length mm	Critical Aspect Ratio l_c/d mean	99% confidence limits on the mean
none	0.74	108	101-115
THF extraction	0.88	130	122-135
heated at 750°C	0.71	100	---

COMPARISON OF AS4, AS1 AND XAS

The surface (and other) properties of the three carbon fibers, AS1, AS4 and XAS were studied to try to find a reason for the difference in their adhesion to the thermoplastics.

SCANNING ELECTRON MICROSCOPY (SEM) The three fibers were examined using SEM and the results are presented in Fig 25 The XAS fiber has a highly striated surface grooves and ridges approximately parallel to the fiber axis. Although these grooves may enhance adhesion to a matrix, they do not explain the greater adhesion to the thermoplastics compared to AS1 and AS4. The AS1 has a very similar striated surface yet the critical lengths and birefringence patterns indicated the adhesion of the AS1 to be as low as for the smooth AS4 The AS1 and XAS have similar surface topography since they are manufactured from the same Courtaulds PAN precursor

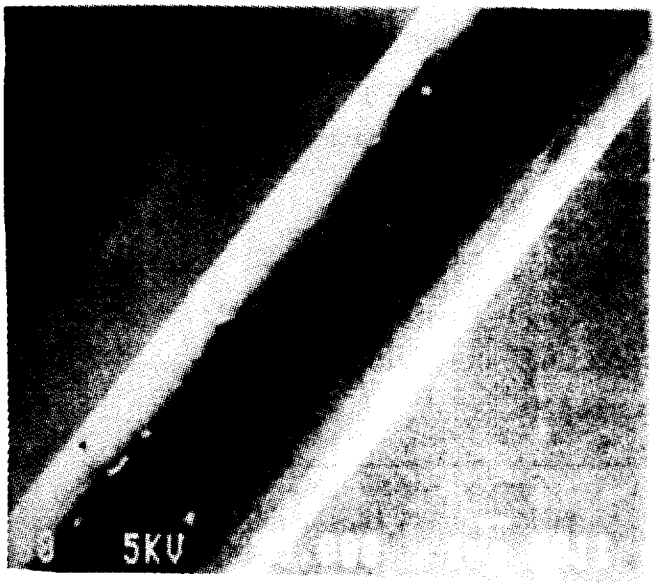

AS4
LOW ADHESION

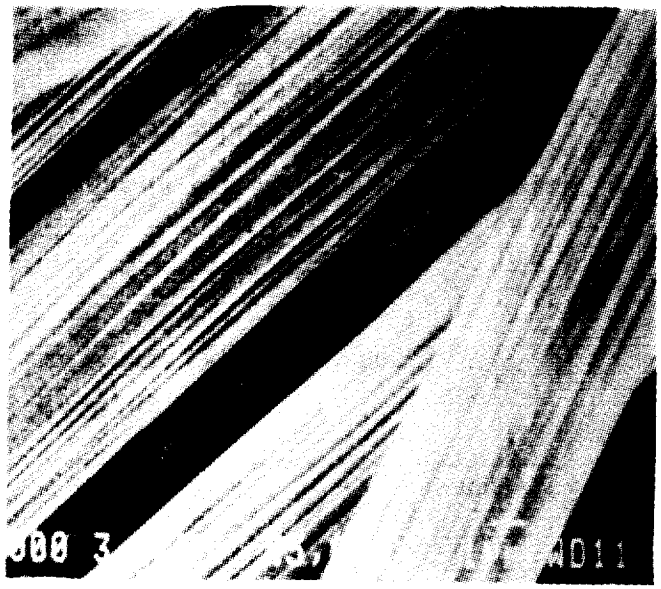

XAS
HIGH ADHESION

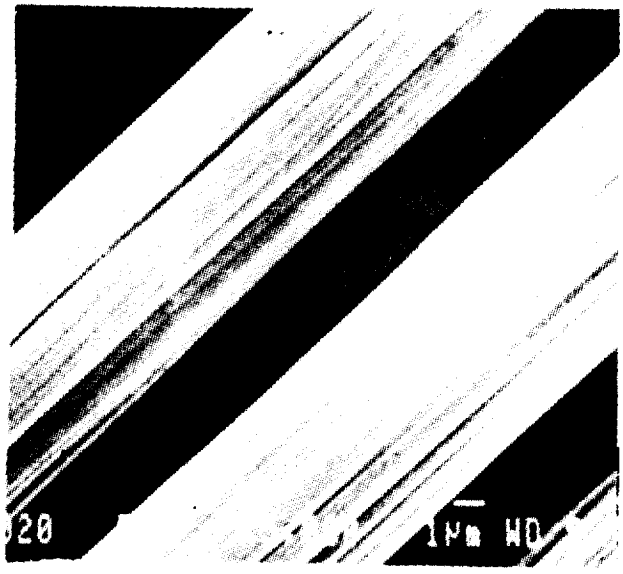

AS1
LOW ADHESION

Figure 25 SEM photomicrographs of AS1, AS4 aand XAS

X-RAY PHOTON SPECTROSCOPY (XPS) Surface analysis of the AS4 and XAS fibers revealed a significant difference in surface chemical composition. The results are presented in Table XII as the elemental composition of the surface to a depth of approximately 10nm, expressed in atomic percent

TABLE XII

XPS ANALYSIS

FIBER	ELEMENTAL COMPOSITION,% C	O	N
AS4	90	5.7	4.3
XAS	84	7.6	8.4

The XPS spectra were deconvoluted for specific surface groups. The results are presented in Table XIII

The data in Tables XII and XIII were obtained on only one sample each of AS4 and XAS so there is a question as to the statistical significance of the differences in composition. However, a measure of the compositional variance was obtained in a multiple sample analysis of AS4 done under Hercules IR&D funding. Six samples from three different production lots of fiber were analyzed for a total of 18 spectra. The average oxygen and nitrogen elemental composition are given in Table XIV along with the standard variation (SD) for the different lots and for the total sampling. Using "3-sigma" as an index of significant difference and applying it to the data in Table XII, the difference in the oxygen composition between AS4 and XAS is not significant but there is a significant difference between the nitrogen compositions [***]

[***] XPS analysis of the fiber tows used in this study indicate that the difference in oxygen composition in Table XIV *is* significant. These analyses were done since the end of this Contract

TABLE XIII

DECONVOLUTION OF XPS SPECTRA

MOLECULAR GROUP	AS4	XAS
	percent	
-COOH	--	present
-C=O	2.4	4.3
-COX -COC -COR	2.8	3.6
-COH	0.6	--
heterocyclic N	1.6	3.6

TABLE XIV

Variance in XPS Chemical Analysis of AS4 Fiber

Sample	Elemental Composition[a]			
	O(1s)		N(1s)	
	mean	SD	mean	SD
lot A (6 samples)	9.15	1.14	6.32	0.52
lot B (6 samples)	7.53	0.36	6.67	0.27
lot C (6 samples)	9.47	1.81	6.55	0.80
total (18 samples)	8.71	1.58	6.51	0.59

a. based on 100% carbon

WETTABILITY MEASUREMENTS The contact angle measurements made using the Wilhelmy tensiometer were highly erratic for each sample and from one sample to the next. Representative results are presented in Table XV. There is the expected

TABLE XV

Contact Angle Data

Liquid	Surface Tension dynes/cm	Contact Angle, deg Advancing θ_A	Receding θ_R
	AS4		
hexadecane	27.6	0	0
α - bromonapthalene	44.6	29	26
α - bromonapthalene	44.6	12	0
diiodomethane	50.8	36	0
water	72.8	57	31
water	72.8	70	25
	XAS		
hexadecane	27.6	0	0
α - bromonapthalene	44.6	42	0
α - bromonapthalene	44.6	22	0
diiodomethane	50.8	28	0
water	72.8	55-59	24

trend of increasing contact angle with increasing surface tension of the wetting liquids. The hysteresis (difference between advancing and receding angles) is very large especially for XAS. This hysteresis is undoubtedly due to chemical heterogeneity for both types and to surface roughness especially in the case of the XAS fiber. Two tensiometer traces are presented in Figs. 26 and 27 for AS4 wetted by hexadecane and water respectively. The hexadecane gave a relatively smooth trace and a calculated contact angle of zero. The water gave a very "noisy" trace with an average advancing angle of about 68° and receding angle of about 25°.

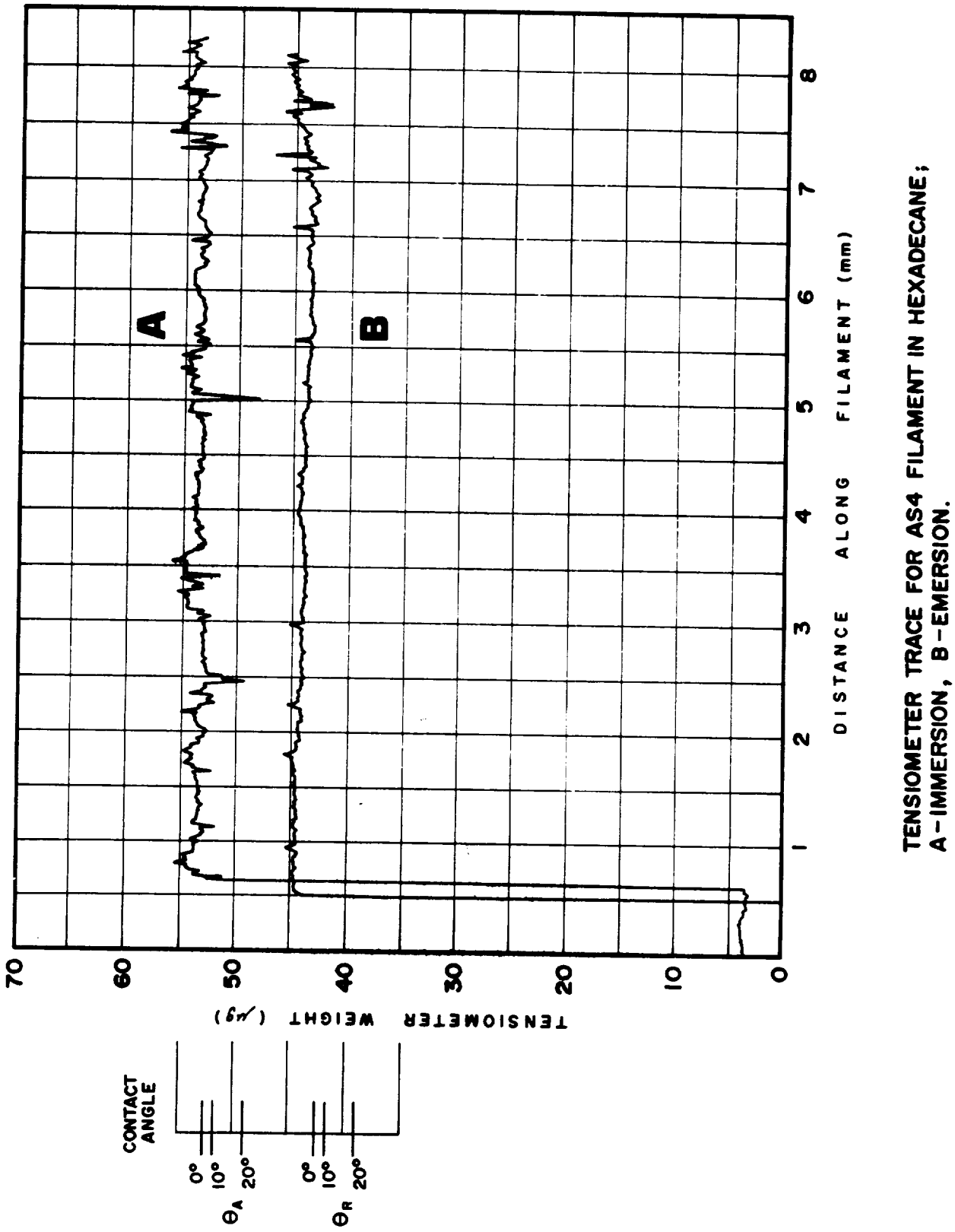

Figure 26. Wetting tensiometer traces for hexadecane on AS4

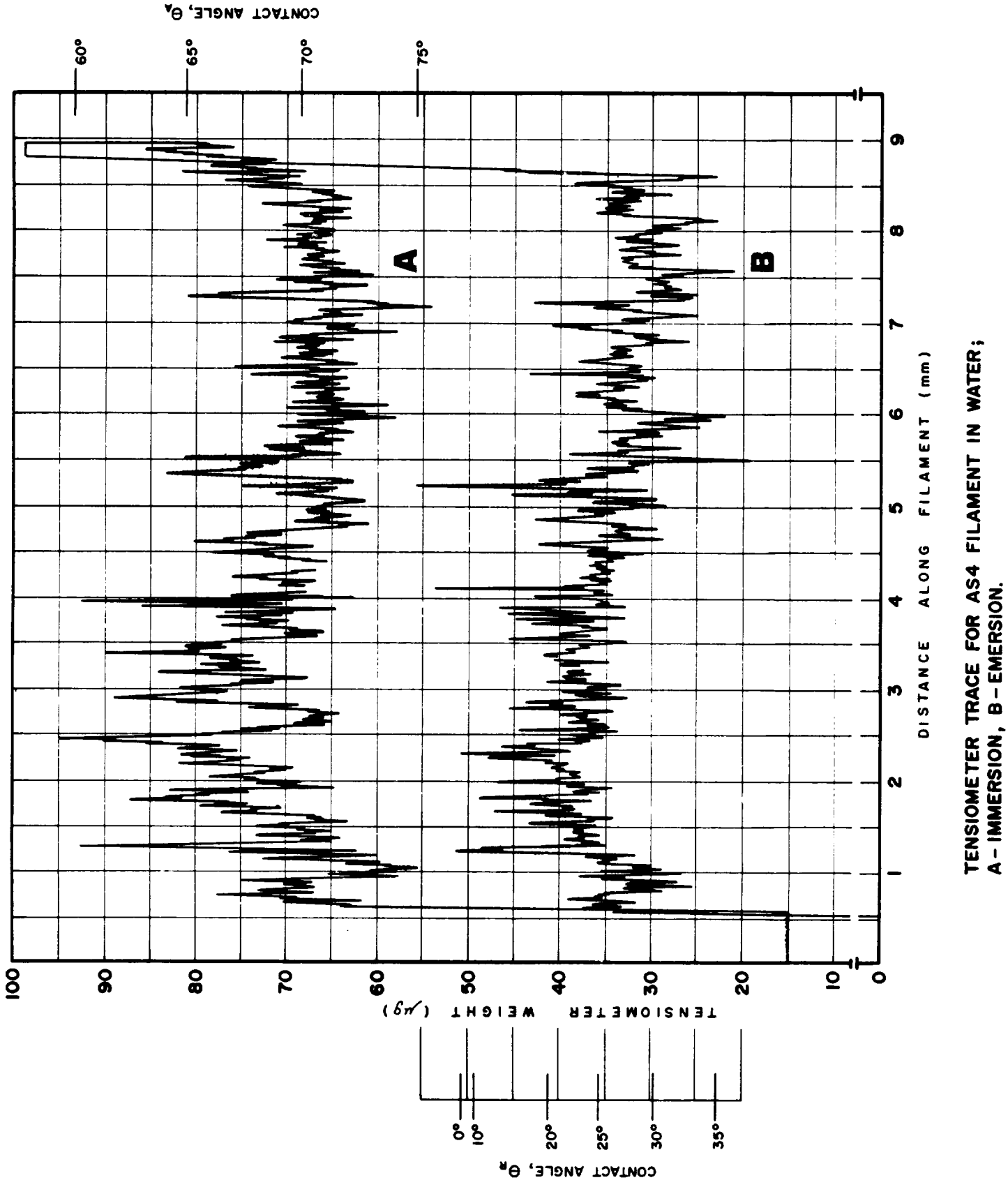

Figure 27 Wetting tensiometer traces for water on AS4

The high frequency oscillations of the tensiometer trace in Fig. 27 are typical of the results for liquids exhibiting finite contact angles. These oscillations are due to the microheterogeneity of the carbon surface and the wetting perimeter changing shape to accommodate to submicron regions of different chemical constitution as shown schematically in Fig 28

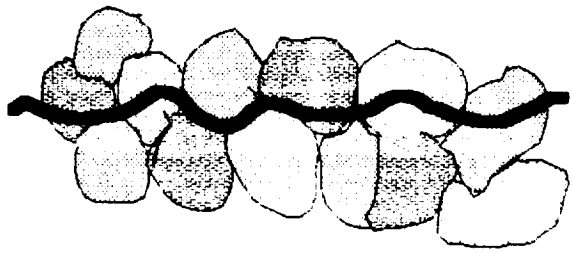

Figure 28 Schematic of the perturbation of the wetting perimeter by patch-wise microheterogeneities

The force measured by the tensiometer is directly related to the length of the wetting perimeter which is changing continuously as the fiber is immersed and emersed through the liquid surface.

This "microhysteresis" has been the subject of theoretical studies of wetting behavior notably by deGennes (19) and Garoff (20). In principle, an analysis of the tensiometer oscillations could yield information about the size and distribution of the heterogeneities and possibly about the difference in their chemical constitution. However, wetting studies of surfaces with known model microheterogeneities are needed before these oscillations can be meaningfully interpreted.

The fiber diameter can be determined when the contact angle is zero and the surface tension of the wetting liquid is known. Under these circumstances, Eq. 6 can be rewritten to:

$$d = ma/\gamma_{LV}$$

Fiber diameters for AS4 and XAS determined using hexadecane ($\theta = 0^0$) are listed in Table XVI

TABLE XVI
Fiber Diameters, μm

	AS4	XAS
	6.92	6.68
	6.42	6.61
	6.70	
	7.09	
	7.09	
ave	6.84 +/- 0.26	6.64

The data are for fibers taken from the same fiber spool and so do not reflect possible variations between spools in the same lot or between production lots Note that there is not a large difference between the diameters of the two fibers despite the roughness of the XAS surface

FTIR ANALYSIS Tows of AS4 and XAS were examined using photo-acoustic FT-IR spectroscopy There were no significant differences in the spectra and as might be expected the spectra were relatively featureless.

THERMAL DESORPTION/MASS SPECTROSCOPY: Volatile products on AS4 and XAS were analyzed by programed heating of fiber samples up to 310°C at a heating rate of 25°C/min with a hold of 5min at 310°C The products were analyzed using mass spectroscopy for total organics and at mass 44, 57 and 149 which correspond to CO_2, straight chain hydrocarbon, and carbonyl fragments respectively The results are presented in Table XVII The total evolution from the XAS was nearly 3X that of the AS4

TABLE XVII

Thermal Desorption Analysis

Fiber	Evolution, mass counts			
	total	mass 44	mass 57	mass 149
AS4	98,175	18,518	5,019	4,623
XAS	317,695	47,435	9,086	1,163

Also there was significantly greater evolution of CO_2 and straight chain hydrocarbon from the XAS than from the AS4. The evolution from AS4 at mass number 149 (presumably carbonyl fragments) was greater for XAS

It is very likely that much of the evolved material came from the interior and not just from the surface As is evident from the data in Table XVII, the fragments analyzed at the three mass numbers represent only a fraction of the material evolved The release of material was essentially continuous during the heat up and hold step except for mass number 149 from the AS4 which peaked at about 210°C and then declined to essentially zero as the sample reached 310°C

CONCLUSIONS

The results presented here indicate low adhesion of the AS1 and AS4 to the thermoplastic polymers compared to the adhesion of these fibers to epoxy polymers The primary evidence for this conclusion is the higher critical lengths for the fibers in the thermoplastics compared to the epoxys and the difference in the stress birefringence at fiber breaks. The birefringence patterns of the AS1 and AS4 in the thermoplastics were characteristic of low adhesion and in fact suggested an easy, "unzipping" of the interface

The results for the XAS fibers indicated strong adhesion in both epoxys and thermoplastics This conclusion is based on the short critical lengths and the birefringence patterns at fiber breaks

The evidence for strong adhesion of the XAS to the thermoplastics actually supports the conclusion of low adhesion of AS1 and AS4 in that it removes the possibility that the results for the AS fibers were in some way related to the different methods of specimen preparation

None the less, there is a fundamental difference in specimen preparation for the epoxy polymers compared to the thermoplastics in that the epoxy specimens were heat cured which produced a compressive stress due to thermal contractions on cool down to room temperature However, as discussed in Appendix A, the drying temperature used to prepared the thermoplastic specimens produced about the same compressive stress as for the epoxy specimens Consequently the lower adhesion of the AS1 and AS4 fibers cannot be attributed to differences in thermal compressive stress.

Attempts to determine the reasons for the difference in adhesion of XAS compared to AS1 and AS4 were unsuccessful Surface roughness was not a factor nor was there any evidence of a weak boundary layer The XPS analysis revealed a difference in the chemical composition of the surface of XAS compared to AS4 but no obvious reason for the low adhesion of AS4 to such chemically different polymers

FUTURE WORK

The reason for the difference in adhesion of XAS and AS4 to thermoplastics needs to be resolved Once understood it will provide insights into the factors that determine adhesion between carbon fibers and organic polymers

There does not seem to be any specific chemical reason for the differences The XAS and AS4 exhibited distinctly different adhesion strengths to very chemically different polymers Only in the case of the thermosetting polymers - the epoxys- was the adhesion strong for both XAS and AS4 (and also AS1). This fact raises the issue of polymer conformation at the interface The epoxy structure forms by chemical reaction of the epoxide and curative more or less independent of the chemical constitution of the fiber surface The conformation of a thermoplastic, whether applied from a solvent or as a melt, can be quite sensitive to the chemical environment The XPS analysis suggests that the XAS and AS4 surfaces are chemically different and this difference may be such that all of the thermoplastics adsorb on the XPS in configurations that favor strong bonding This rather speculative hypothesis implies a specific difference in the chemical constitution of the fibers that is not evident from

the XPS data. Quite possibly, it is not the difference in chemical composition but in the spacial distribution of chemical groups that affect conformation.****

Experimental studies of polymer conformation on carbon fiber surfaces present some formidable difficulties. Perhaps adsorption studies of model polymers should be considered. Before doing so however there should be a more thorough chemical characterization of the carbon fiber surface using XPS (because of its surface specificity) including derivitization studies to confirm the presence of chemical groups presumed from the deconvolution of XPS spectra. Deconvolution involves assumptions that can be very tenuous in discriminating between similar chemical specie, e.g., carbon-oxygen moieties, and chemical specie at low concentrations.

Wetting tensiometric measurements are also very surface specific and are clearly very sensitive to chemical heterogeneity. However the interpretation of tensiometer results poses some formidable problems.

The difference in the adhesion behavior of XAS, AS4 and AS1 may be due to differences in the mechanical properties of the fiber surfaces rather than to chemical differences. Roselman and Tabor (21) determined the sliding friction of single carbon filaments and found a very low surface shear strength. They suggested that the outer surface region (first few nanometers) behaved more like a highly viscous liquid (a highly defective solid). This observation is not especially surprising considering the molecular structural changes and gas evolution during carbonization and graphitization. These friction tests should be repeated for XAS and AS4 not only as part of an effort to understand the adhesion differences but also for the implications of such a shear sensitive layer to the behavior of carbon fiber reinforced composites in general.

An issue not addressed in this study is fiber-fiber interaction. In any investigation using the embedded single fiber test there is always the question of how the results would be influenced by neighboring fibers. In order to study this question a device was constructed as part of this Contract to align 2-5 filaments in close

---

**** The possible role of polymer surface configuration in the adhesion of the thermoplastics was suggested to the author by Prof. L.T. Drzal, Michigan State University and Dr. T. M. Johnson, Phillip Petroleum Co., Bartlesville, OK.

proximity so that they can be embedded in epoxy or thermoplastic polymers using the same techniques described for single fibers

The multiple fiber alignment device is shown in Fig 29 mounted on a stereomicroscope The filaments are strung between the pins of two combs that can be rotated in unison The insert in Fig 29 is a photomicrograph of five filaments aligned using the device and embedded in an epoxy polymer The desired spacing between fibers is one filament diameter or less which the photomicrograph shows was not achieved However, this was a first effort that can be improved with more operator experience

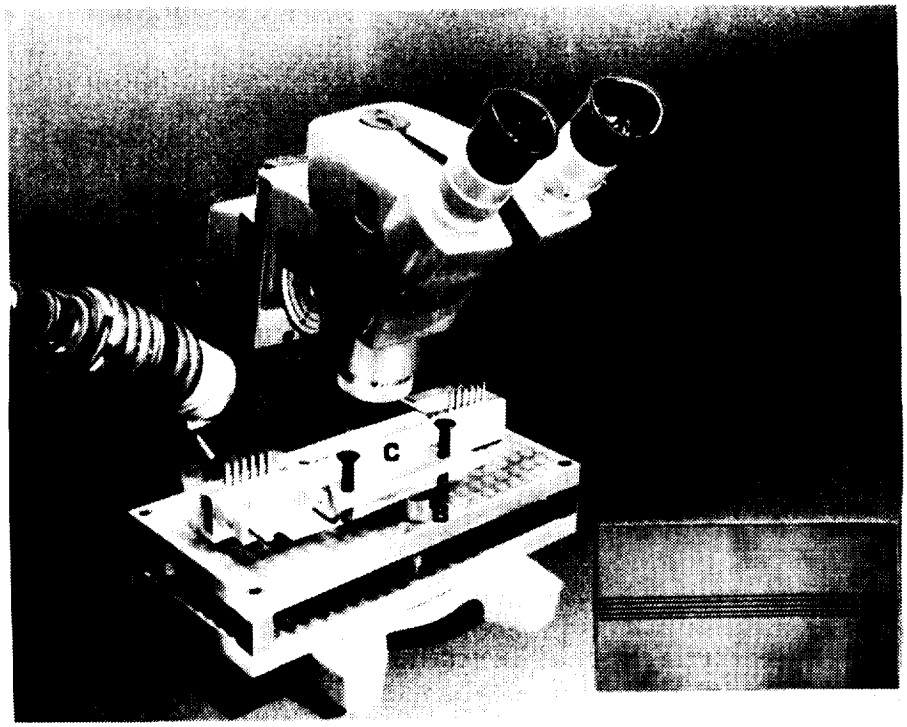

Figure 30 Apparatus for aligning multiple (2-5) filaments A combs B knob used to rotate combs C mold in which the filaments are aligned and then embedded

ACKNOWLEDGEMENTS

The author wishes to thank Dr Jeffrey Hinkley Dr Norman Johnston (NASA Langley), Mr Niel Hansen, and Mr David Boll (Hercules Aerospace) for very helpful advice and discussions during the course of this work The skill and patience of Mr Larry Cordner (Hercules) who conducted the experimental work on this Program are gratefully acknowledged along with the efforts of Mr Merwin Jensen (Hercules) who

designed the microtensile tester and multiple fiber alignment device Finally, special thanks to Mr John Weidner (Hercules) for his continued encouragement

REFERENCES

1 Leach, D C , Curtis, D C , and Tamblin, D R , "Delamination Behavior of Aromatic Polymer Composite, APC 2," ASTM Symposium on Toughened Composites, Houston, March 13-15, 1985

2 Bascom, W D , "Fractographic Analysis of Interlaminar Fracture," ASTM Symposium on Toughened Composites, Houston, March 13-15, 1985

3 Bascom, W D , Timmons, C O , and Jones, R L , "Apparent Interfacial Failure in Mixed-Mode Adhesive Fracture," J Mat Sci , 10 1037 (1975)

4 Bascom, W D , Boll, D J , Fuller, B , and Phillips, P J , "Fractography of the Interlaminar Fracture of Carbon-Fiber Epoxy Composites," J Mat Sci , 20 3184 (1985)

5 Piggott, M R , Sanadi, A , Chua, P S , and Andison, D , "Mechanical Interactions in the Interphasial Region of Fibre Reinforced Thermosets," in Composite Interfaces, H Ishida and J L Koenig, Eds , North-Holland, New York, 1986, p 109

6 Cox, H L , "The Elasticity and Strength of Paper and Other Fibrous Materials," Brit J Appl Phys , 3 72 (1952)

7 Kelly, A , and Tyson, W R V , "Tensile Properties of Fibre-Reinforced Metals, Copper/Tungsten and Copper/Molybdenum," Mech & Phys of Solids, 13 329 (1965)

8 Hedgepeth, J M , and Van Dyke, P , J Comp Mat , 1 294 (1967)

9 Kelly, A , Strong Solids, 2nd Ed , 1973, p 172

10 Fraser, W A , Ancker, F H , and DiBenedetto, A T , "A Computer Modeled Single Filament Technique for Measuring Coupling and Sizing Agent Effects in Fiber Reinforced Composites," Proc Conf on Reinforced Plastics, Soc Plastics Ind , 1975, Section 22A, p 1

11 Fraser, W A , Ancker, F H , DiBenedetto, A T , and Elbirli, B , "Evaluation of Surface Treatments for Fibers in Composite Materials," Polym Comp , 4 238 (1983)

12 Drzal, L T , Rich, M J , and Lloyd, P F , "Adhesion of Graphite Fibers to Epoxy Matrices, I, The Role of Fiber Surface Treatment," J Adhesion, 16 133 (1983)

13 Drzal, L T , Rich, M J , Koenig, M F , and Lloyd, P F , "Adhesion of Graphite Fibers to Epoxy Matrices, II, Effect of Fiber Finish," J Adhesion , 16 133 (1982)

14 Bascom, W D , and Jensen, R M , "Stress Transfer in Single Fiber/Resin Tensile Tests," J Adhesion, 19 219 (1986)

Fracture in Single Fiber/Epoxy Composites", in Composite Interfaces. H. Ishida and J.L.Koenig, Eds., North-Holland, New York, 1986, p.109

16. Marsh, D. M., Micro-tensile Testing Machine, J. Sci. Instr., 38 229 (1961)

17. Whitney, J. M., and Drzal, L.T., "Three Dimensional Stress Distribution Around an Isolated Fiber Fragment." ASTM Symposium on Toughened Composites, Houston, March 13-15, 1985

18. Bascom, W. D., and Drzal, L.T., "The Surface Properties of Carbon Fibers and Their Adhesion to Organic Polymers. NASA CR-4084, July 1987.

19. de Gennes, P. G., "A Model for Contact Angle Hysteresis." Rev. Mod. Phys., 57 827 (1985)

20. Schwartz, L. W., and Garoff, S., "Contact Angle Hysteresis and the Shape of the Three-Phase Line." J. Colloid and Interface Sci., 106 422 (1985)

21. Roselman, I.C., and Tabor, D., "The Friction of Carbon Fibres," J. Phys. D: Appl. Phys. 9 2517 (1976)

APPENDIX A

RADIAL COMPRESSIVE STRESS ON A SINGLE EMBEDDED FILAMENT

W. D. Bascom
S. Wong
and
E. Wall

Materials Science and Engineering Department
University of Utah

Whitney and Drzal* have developed an analytical model for predicting the stress on an isolated broken fiber embedded in an unbounded matrix. Their analysis includes the effect of thermally induced stresses that result from curing or drying at an elevated temperature and then cooling to 25°C. The stresses of interest here are the radial compressive stresses which enhance the inherent adhesive strength between fiber and matrix.

The pertinent equations are:

$$\sigma_r = \{ A_2 + \mu^2 A_1 (4.75x - 1) e^{-4.75x} \} \varepsilon_0$$

$$\bar{X} = x/\ell$$

$$A_1 = E_{1f} (1 - \varepsilon_{1f}/\varepsilon_0) + (4K_f G_m \nu_{12f})/(K_f + G_m) \{ \nu_{12f} - \nu_m + [(1+\nu_m)\varepsilon_m - \nu_{12f}\varepsilon_{1f}]/\varepsilon_0 \}$$

$$A_2 = 2K_f G_m/(K_f + G_m) \{ \nu_{12f} - \nu_m + [(1+\nu_m)\varepsilon_m - \varepsilon_{2f} - \nu_{12f}\varepsilon_{1f}]/\varepsilon_0 \}$$

$$\varepsilon_m = \alpha_m \Delta T, \quad \varepsilon_{1f} = \alpha_{1f} \Delta T, \quad \varepsilon_{2f} = \alpha_{2f} \Delta T$$

$$\mu = \sqrt{G_m/E_{1f} - \nu_{12f} G_m}$$

$$K_f = E_m/2(2 - E_{2f}/2G_{2f} - 2\nu_{12f}E_{2f}/E_{2f})$$

The radial σ_r stress is normalized by the far field stress σ_0.

$$\sigma_0 = A_3 \varepsilon_0$$

$$\varepsilon_0 = 0.01\%$$

$$A_3 = E_{1f} + 4K_f \nu_{12f} G_m (\nu_{12f} - \nu_m)/(K_f + G_m)$$

---

* Whitney, J. M. and Drzal, L. T., "Three Dimensional Stress Distribution Around an Isolated Fiber Fragment," ASTM Symposium on Toughened Composites, Houston, March 13-15, 1985.

The normalized radial compressive stress, σ_r / σ_o, was calculated for AS4 carbon fiber in the DGEBA/m-PDA epoxy for $\Delta T = -75^oC$ and in polycarbonate for $\Delta T = -50^oC$, -95^oC, and -175^oC. The material constants used are listed in Table IA and IIA. The constants for the fiber and the epoxy were taken from the Whitney and Drzal paper and the data for polycarbonate were obtained from various literature sources.

TABLE IA
Matrix Material Constants

	epoxy	polycarbonate
G_m	1.4GPa	0.790GPa
E_m	3.8GPa	2.4GPa
ν_m	0.35	0.35
α_m	$68 \times 10^{-6}/^oC$	$67.5 \times 10^{-6}/^oC$
ε_m		
-75°C	-5.1×10^{-3}	
-50°C		-3.4×10^{-3}
-95°C		-6.4×10^{-3}
-175°C		-1.18×10^{-3}

TABLE IIA

Fiber Material Constants

E_{1f}	241GPa
G_{2f}	8.3GPa
E_{2f}	21GPa
ν_{12f}	0.25
α_{1f}	$-0.11 \times 10^{-6}/^oC$
α_{2f}	$8.5 \times 10^{-6}/^oC$

ε_{1f}

-50°C	5.5×10^{-6}
-75°C	8.2×10^{-6}
-95°C	10.4×10^{-6}
-175°C	19.2×10^{-6}

ε_{2f}

-50°C	-4.2×10^{-4}
-75°C	-6.4×10^{-4}
-95°C	-8.1×10^{-4}
-175°C	-14.9×10^{-4}

The radial compressive stresses from the fiber end $\bar{x}=0$ to the far field value $\bar{x}=1$ are plotted for the epoxy matrix in Fig. 1A and for the polycarbonate matrix in Fig. 2A

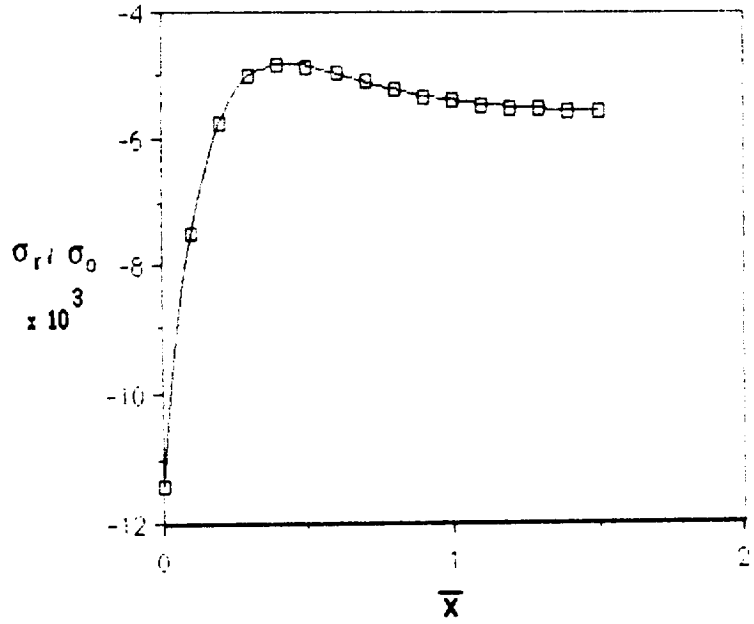

Figure 1A Interfacial radial stress for carbon fiber/epoxy matrix. $\Delta T = -75°C$

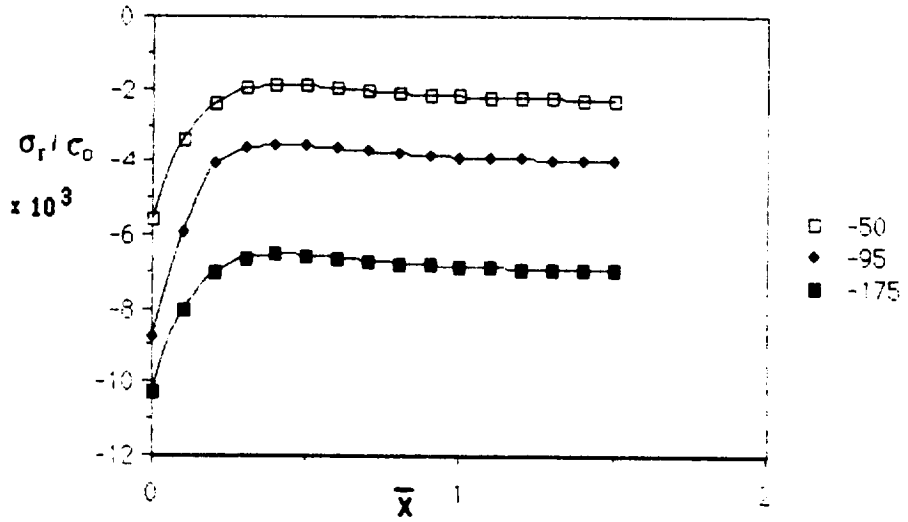

Figure 2A. Effect of cooling temperature on the interfacial radial stress for AS4/ polycarbonate

In Table IIIA the far field (x = 1 5) radial stresses are listed along with experimental ℓ_c/d values including data for AS4/polycarbonate specimens dried at 75°C, 120°C and 200°C The comparison suggests that for the drying temperature used in preparing the thermoplastic specimens (75-81°C) the radial compressive stress was 40% of the stress on the fiber in the epoxy matrix Actually the stress on the fiber in the polycabonate was probably less than calculated due to molecular relaxation Only on cooling from 200°C (ΔT = 175°C) was the radial stress on the fiber in polycarbonate comparable to the stress in the epoxy

TABLE IIIA

Effect of Cooling on Radial Stress and Critical Aspect Ratio

Matrix	ΔT(°C)	$\sigma_r/\sigma_o x10^{3a}$	ℓ_c/d [b]
DGEBA/mPDA	-75	5 5	55
polycarbonate	-50	2 3	108
polycarbonate	-95	4 0	71
polycarbonate	-175	7 0	64

a at $\bar{x}$ = 1 5

b AS4 fiber

Thermally induced radial compression stresses present an inherent difficulty in using the embedded single fiber test to measure fiber/matrix bond strength. Any heating and cooling in specimen preperation induces a compressive stress that cannot be fully separated from the actual bond strength. The analysis used here does not account for stress relaxation. Ideally a specimen should be prepared and tested at the same temperature. Relative comparisons of bond strength should be done with specimens that had thermal histories that produce the same radial stress.

Compressive stress effects do not alter the principle conclusion of this study: the large difference in the adhesion of AS4 (and AS1) compared to XAS to the thermoplastic polymers. All of the thermoplastic specimens were dried at 75°C or 81°C.

Standard Bibliographic Page

1. Report No.	2. Government Accession No.	3. Recipient's Catalog No.
NASA CR-178306		

4. Title and Subtitle	5. Report Date
Interfacial Adhesion of Carbon Fibers	August 1987
	6. Performing Organization Code
7. Author(s)	8. Performing Organization Report No.
Willard D. Bascom	
9. Performing Organization Name and Address	10. Work Unit No.
Hercules, Inc. Hercules Aerospace Division Magna, UT 84044	505-63-01-01
	11. Contract or Grant No.
	NAS1-17918
12. Sponsoring Agency Name and Address	13. Type of Report and Period Covered
National Aeronautics and Space Administration Washington, DC 20546-0001	Contractor Report
	14. Sponsoring Agency Code

15. Supplementary Notes

Use of trade names or names of manufacturers in this report does not constitute an official endorsement of such products or manufacturers, either expressed or implied, by the National Aeronautics and Space Administration.
Langley Technical Monitor: J. A. Hinkley
Final Report - November 1984 - October 1986

16. Abstract

Relative adhesion strengths between AS4, AS1, and XAS carbon fibers and thermoplastic polymers were determined using the embedded single filament test. Polymers studied included polycarbonate, polyphenylene oxide, polyetherimide, polysulfone, polyphenylene oxide blends with polystyrene, and polycarbonate blends with a polycarbonate-polysiloxane block copolymer. Fiber surface treatments and sizings improved adhesion somewhat, but adhesion remained well below levels obtained with epoxy matrices. An explanation for the differences between the Hercules and Grafil fibers was sought using XPS, wetting, SEM, and thermal desorption analysis.

17. Key Words (Suggested by Authors(s))	18. Distribution Statement
Carbon fibers Fiber/matrix adhesion Organic matrix composites Thermoplastics	Unclassified - Unlimited Subject Category 24

19. Security Classif.(of this report)	20. Security Classif.(of this page)	21. No. of Pages	22. Price
Unclassified	Unclassified	52	A04

For sale by the National Technical Information Service, Springfield, Virginia 22161